Self-Contact Preventing Energy for Tubular Rods

Journal of Nonlinear Science (2025) 35:34
https://doi.org/10.1007/s00332-025-10128-9

Journal of Nonlinear Science

# Self-Contact Preventing Energy for Tubular Rods

**Chiara Lonati**[1] · **Alfredo Marzocchi**[1]

Received: 9 June 2024 / Accepted: 3 January 2025 / Published online: 23 January 2025


**Abstract**
We introduce a generalization of Möbius energy for knots to an energy functional for tubular neighbourhoods of closed inextensible curves. We prove the continuity of the energy and its boundedness for physically admissible tubes without self-contact and in particular for the torus. The functional allows to distinguish isotopy classes of the centreline through its physical resemblance to a self-repulsive electrostatic energy. If the tube has zero thickness, O'Hara's functional is recovered. Finally, a discussion on the possible exponents in the functional is carried out and numerical examples are studied to highlight some advantages of our new definition.

**Keywords** Self-contact · Interpenetration of matter · Möbius energy · Tubular neighbourhoods

**Mathematics Subject Classification** 57K10 · 70G75 · 74K10 · 74M15

## 1 Introduction

In the theory of knots (Adams 1994; Burde and Zieschang 2003; Crowell and Fox 2012), it is customary to introduce configurations avoiding self-intersection points, the so-called multiple points. This is both a requirement and a necessary condition to subdivide all possible configurations into disjoint classes, named ambient isotopy classes, and it copes with the physical intuition.

For this reason, O'Hara (1991) defined an energy functional on a knot based on a sort of electrostatic potential called *Möbius energy*, which prevents self-intersections distinguishing different types of knots and that was proved (Freedman et al. 1994) to generate a minimum energy configuration on any prime knot class, where a sort

Communicated by Eliot Fried.

✉ Chiara Lonati
chiara.lonati@unicatt.it

Alfredo Marzocchi
alfredo.marzocchi@unicatt.it

[1] Dipartimento di Matematica e Fisica "N. Tartaglia", Università Cattolica del Sacro Cuore, via della Garzetta 48, I-25133 Brescia, Italy

of "optimal distance with itself" is obtained. Though not properly physical (the case of real electrostatic energy was not contemplated in the theory), O'Hara ideas were very fruitful and led to many further results, like the fact that the circle actually reaches the absolute minimum and the proof of the existence of a minimum energy configuration of the knot in each isotopy class (Freedman et al. 1994), in addition to some generalizations of Möbius energy for knots and the study of minimizers for its coupling with an elastic energy on the knot (O'Hara 1992, 1994, 2008; Kim and Kusner 1993; Buck and Orloff 1995; Simon 1996; Mosel 1998).

More in detail, O'Hara's functional contains a term $1/|x-y|^\alpha$, where $|\cdot|$ is the Euclidean distance between points on the knot, which diverges as $x$ approaches $y$, subtracted by a term $1/d(x,y)^\alpha$ where $d$ is the distance between $x$ and $y$ on the knot, which diverges too as $x$ approaches $y$. Nevertheless, the difference is convergent as $x \to y$, so that it is possible to integrate it over all possible couples of points on the knot and, when there are no multiple points, get a finite integral. When the knot has multiple points, however, $|x-y| \to 0$ but $d(x,y)$ does not, so that the integral diverges and hence a knot with multiple points cannot be a minimizer. The exponent $\alpha$ must belong to a precise interval in $\mathbb{R}$ to have a well-defined energy for knots. For $\alpha = 1$, one obtains the classical Coulomb electrostatic potential that however does not seem to provide minimizers for O'Hara's functional.

The aim of this paper is to generalize some features of O'Hara's theory to three-dimensional objects which are "close" to a knot, hopefully easier to use for real physical experiments and more suitable for applications, like modelling of proteins or DNA folding or the description of charged filaments. In many problems involving deformable rods (Antman 2005; Schuricht 2002; Gonzalez et al. 2002; Schuricht and Mosel 2003; Chamekh et al. 2009) as well as filaments joint with minimal surfaces, the so-called Kirchhoff-Plateau problem (Giusteri et al. 2016, 2017; De Rosa and Lussardi 2022; Bevilacqua et al. 2018, 2019, 2020; Ballarin et al. 2024; Bevilacqua and Lonati 2023), an appropriate choice of the elastic energy term leads to the existence of a minimum energy configuration, but non-interpenetration of matter must be imposed implicitly on the space of all configurations. Many studies were carried out to express non-interpenetration and self-contact conditions for elastic loops (Lonati and Marzocchi 2024), both from a local point of view, (Chamekh et al. 2009; Mlika 2018; Chamekh et al. 2020) and from a global one, where the formulation does not involve quantities described through local geometric quantities, as for example in Ciarlet and Nečas (1987), Gonzalez et al. (2002), Schuricht (2002). However, it is almost impossible to perform a priori numerical experiments on the solution, since the space of admissible configurations depends on possible points of contact, i.e. on the solution itself. A theory in which impossibility of interpenetration is automatically necessary would be welcome at least in this sense.

A variety of studies deepens the notion of "thickness" of a knot: in Gonzalez and Maddocks (1999), Schuricht and Von der Mosel (2004) this concept is related to the notions of ideal knot and global radius of curvature and in Mosel (1999) a small thickness is assigned to a knot in form of an obstacle, in order to minimize the curvature functional on separated isotopy classes. In Kusner and Sullivan (1998), Litherland et al. (1999), the thickness is related, as in O'Hara's works, to the distortion and the so-called rope length of a knot. In addition, several generalizations of O'Hara's ideas

were carried out in the last decades, both for minimization procedures, regularity of minimizers, study of the energy for generic manifolds in different dimensions and codimensions (Kusner and Sullivan 1994). In particular, results in this last sense can be found in Käfer and von der Mosel (2023), O'Hara (2023). A tentative generalization of O'Hara's approach was carried out in Rawdon and Simon (2002); however, there the thickness of the knot is not considered in the formulation of the energy, but is used to find bounds for Möbius energy. An interesting general approach for three-dimensional surfaces is proposed in Kusner and Sullivan (1994); differently from Kusner and Sullivan (1994), that appears quite difficult to be expressed by geometric quantities of the object, we want here to explicitly describe the functional using the non-vanishing thickness of the elastic filament. In addition, we use for the definition of the functional just lengths of curves explicitly defined on the boundary of the object without using further definitions and we want also to give an exact characterization of self-contact points. Many works were done on an energy defined using Menger curvature by Strzelecki and Von Der Mosel starting from Strzelecki and Von Der Mosel (2011), but it seems that the global radius of curvature $\Delta[\gamma]$ of a curve $\gamma$ depends in a non-smooth and nonlinear way on the curve itself, which seems quite demanding for a numerical treatment. However, all these results are mainly developed under a theoretical point of view, and do not provide an explicit formulation depending on the geometric parameters of the object and the thickness, but they study more a possible optimization of the thickness of the object. Moreover, we are more interested in possible applications to real physical problems, rather than on a geometric or topological treatment. We believe that our energy could be useful to implement into numerical codes in order to prevent a priori interpenetration. For this reason, we provide two simple but important examples to show that this happens.

We are thus going to define an energy with two terms, like Möbius energy, that can be added to other energies and provide with minimizers that automatically satisfy non-interpenetration of matter; moreover, for vanishing thickness it will reduce to Möbius energy.

In particular, we will consider only tubular neighbourhoods of closed curves with fixed length, that are a suitable first approximation for inextensible, unshearable, closed Kirchhoff rods, which will be the object of a further study. We deal here with a description of our object based on the Serret–Frenet frame; we underline that, to have a well-defined frame also when the curvature of the centreline vanishes, one could extend the results to the Bishop frame (Bishop 1975; Bevilacqua et al. 2022) without difficulties, as well as considering twist effects.

Three-dimensional objects like tubes of finite thickness have the advantage that overlapping of points appears before their midlines self-intersect and the drawback that they are complicated to treat since the form of the boundary comes into play. Furthermore, there is no easy or apparent equivalent of O'Hara's distance $d(x, y)$ on the surface of the tube which blows up at the same order of the Euclidean distance. This equivalent quantity should of course tend to O'Hara distance as the cross-section of the tube shrinks to its midline, and should be reasonably computable in the easiest case of the torus.

As in O'Hara (1991), where O'Hara partitioned the space of knots into isotopy classes separated by "walls" with infinite Möbius energy, our goal is the possibility of dis-

tinguishing ambient isotopy classes of the centreline of the corresponding tubular neighbourhoods. Moreover, we would like to split them into configurations without self-contact and configurations with self-contact or interpenetration of matter, in order to detect the physically admissible ones. The main improvement from O'Hara's works and its extensions (O'Hara 1991, 1992, 1994, 2008; Kim and Kusner 1993; Freedman et al. 1994; Buck and Orloff 1995; Simon 1996; Mosel 1998) is indeed the introduction of the rod thickness.

In this article, we propose and discuss a function, denoted with $d^*(x, y)$, which meets these two requirements. The function is explicitly defined for a tubular neighbourhood of a closed knot and the functional is shown to be finite if and only if the tube does not present self-contact or interpenetration. Moreover, we compute its value for a torus and show some properties as boundedness, continuity, divergence to infinity only in the case of self-contact or not admissible configurations and we prove that, for a cross-section with vanishing thickness, we recover O'Hara's functional.
Because of the presence of the torsion of the midline in the expression of $|x - y|$ and in the definition of $d^*$, unlike in O'Hara's theory, higher derivatives of the midline are necessary to define the functional. As above, the case $\alpha = 1$ that corresponds to the Coulomb electrostatic potential does not provide a divergent functional.
The plan of the paper is as follows. In Sect. 2 we introduce the model through classical knot theory and we define our object. In Sect. 3 we highlight some geometrical properties of a generic tubular neighbourhood and we define the quantities necessary for the definition of the energy functional. In Sect. 4 we proceed with the definition of the functional and in Sect. 5 we prove the fundamental properties of the model, similar to the ones proved for O'Hara's functional in O'Hara (1991), Freedman et al. (1994). In Sect. 6 we show how one can easily recover the classical Möbius energy and in Sect. 7 we carry out a discussion on the suitable exponent for the terms contained in the functional, finding a result analogous to the one contained in Freedman et al. (1994). Finally, in Sect. 8, we provide two numerical examples that support our results and show the possibility of coupling it with an elastic energy and compute the functional also for the case of a filament with free ends. Moreover, the data suggest also that a complete analysis of the energy as a function of the thickness could be carried out, not only for thin filaments.

## 2 Knot Theory Approach

We start recalling some basic definitions that will be useful in what follows. For the standard definitions on knots, which are embeddings $S^1 \to \mathbb{E}^3$, where $\mathbb{E}^3$ is the usual affine space of points, we refer to Adams (1994), Burde and Zieschang (2003), Crowell and Fox (2012). The main ingredient for a knot theory approach to the problem relies in how to identify if two knots $K_0$ and $K_1$ are of the same type: the ambient isotopy, which is stronger than simple isotopy.
As explained in detail in Burde and Zieschang (2003), two knots can be isotopic although they are different with regard to their knottedness: they are indeed both homeomorphic to the unit circle, and so to each other, because any region where knotting occurs can be contracted continuously to a point. An ambient isotopy, instead,

takes into account also the neighbouring points of the knot in the "movement" from $K_0$ to $K_1$.
An ambient isotopy is intuitively defined as a rearrangement of a knot in $\mathbb{R}^3$ without letting it pass through itself. Thus, as detailed in Adams (1994), p.12, as a simple clarifying example, one is not allowed to shrink a part of the knot to a point. The following definition is contained in Crowell and Fox (2012).

**Definition 1** Two knots $K_0$ and $K_1$ are *ambient isotopic* if there exists an orientation-preserving continuous map $H : \mathbb{E}^3 \times [0, 1] \to \mathbb{E}^3$, such that for every fixed $t \in [0, 1]$ and $x$ a point of the knot, the map $H_t : \mathbb{E}^3 \to \mathbb{E}^3$, $\{x \mapsto H(x, t)\}$ is a homeomorphism, with $H_0 = \mathrm{Id}_{\mathbb{E}^3}$ and $H_1 \circ K_0 = K_1$.

The letter $t$ suggests that $[0, 1]$ can be seen as a sort of "time" interval: indeed, the point $H_t(x)$ traces the path of the point $x$ during the "motion" of the knot from its initial position on $K_0$ to its final position on $K_1$.

**Definition 2** A knot that is parametrized by an arc-length of class $C^1$ is called tame. Every tame knot is ambient isotopic to a polygonal knot.

We will always consider only tame curves, because we will require an even higher regularity.

**Definition 3** A singular knot is a smooth map $f : S^1 \to \mathbb{E}^3$ whose image has multiple points, i.e. there exist at least two arc-lengths $s_1$ and $s_2$ such that $f(s_1) = f(s_2)$.

Let $\mathcal{M}$ be the set of immersions of $S^1$ into $\mathbb{E}^3$ and

$$\mathcal{K} = \{f : S^1 \to \mathbb{E}^3 : f \text{ is an embedding}\}$$

the set of all knots. The set $\Sigma = \mathcal{M} \setminus \mathcal{K}$ is called *discriminant set* and consists of all singular knots. It can be shown (O'Hara 2008) that two knots in $\mathcal{K}$ lie in the same ambient isotopy class if and only if they can be joined by a path in $\mathcal{K}$ that does not intersect $\Sigma$. Therefore, knot types are in one-to-one correspondence with the connected components, called *cells*, of $\mathcal{M}/\Sigma$. We will consider knots of given finite length $L$ and the arc-length describing the knot varying in the interval $[0, L]$. In our treatment we will work with a tubular neighbourhood of the midline curve (that can be considered a knot) to approach the description of closed, inextensible and unshearable rods made in Antman (2005), Schuricht (2002): we consider a closed curve $\gamma$ in $\mathbb{R}^3$ of fixed length $L$ parametrized by the arc-length parameter $s \in [0, L]$. We assume that this curve is of class $C^3([0, L]; \mathbb{E}^3)$, so that the second derivative is well-defined and continuous and that the curvature of $\gamma$ never vanishes, so we have a well-defined standard Serret–Frenet frame $(\boldsymbol{t}, \boldsymbol{n}, \boldsymbol{b})$. The closure conditions read $\gamma(0) = \gamma(L)$, $\boldsymbol{t}(0) = \boldsymbol{t}(L)$, $\boldsymbol{n}(0) = \boldsymbol{n}(L)$, which obviously imply $\boldsymbol{b}(0) = \boldsymbol{b}(L)$.
We will denote a closed circular tubular neighbourhood with radius $r > 0$ of a curve $\gamma$ as the set

$$T_r[\gamma] = \bigcup_{Q \in \gamma} \{P \in \mathbb{E}^3 : |P - Q| \leq r\} \tag{1}$$

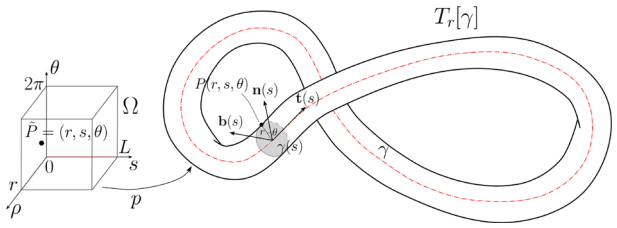


**Fig. 1** Representation of the map $p$ from the set $\Omega$ to $p(\Omega)$. A point $\tilde{P}(r, s, \theta)$ is mapped into $P(r, s, \theta) \in p(\Omega)$. In particular, here $P(r, s, \theta) \in \text{bd}\, T_r$

where $|P - Q|$ is the Euclidean distance between two points in $\mathbb{E}^3$. In the sequel, we will only write $T_r$.
We denote with $p$ the following mapping from a subset of $\mathbb{R}^3$ to a subset of $\mathbb{E}^3$ that associates to $(\rho, s, \theta)$ the point $P$ corresponding to the coordinates $(\rho, s, \theta)$. Any point belonging to $T_r$ obeys

$$p(\rho, s, \theta) - \gamma(s) = \rho \cos\theta\, \boldsymbol{n}(s) + \rho \sin\theta\, \boldsymbol{b}(s). \tag{2}$$

where $s \in [0, L]$, $\rho \in [0, r]$ is the distance from the centreline in the plane determined by $\boldsymbol{n}(s)$ and $\boldsymbol{b}(s)$ and $\theta \in [0, 2\pi]$ is the angle formed with the normal $\boldsymbol{n}(s)$. We notice that thanks to the regularity of $\gamma$ the mapping $p$ turns out to be continuous, surjective and injective if the midline does not present multiple points. We will use the notation $\Omega$ for the set $[0, r] \times [0, L] \times [0, 2\pi]$ and so $p(\Omega)$ will describe the shape of the tube in space.
The boundary $\text{bd}\, T_r$ of $T_r$ is the set of points where $r > 0$ is fixed:

$$\text{bd}\, T_r = \{P = \gamma(s) + r \cos\theta \boldsymbol{n}(s) + r \sin\theta \boldsymbol{b}(s), s \in [0, L], \theta \in [0, 2\pi]\} \tag{3}$$

while the interior part $\text{int}\, T_r$ of $T_r$ is clearly the set of points

$$\text{int}\, T_r = \{P = \gamma(s) + \rho \cos\theta \boldsymbol{n}(s) + \rho \sin\theta \boldsymbol{b}(s), \rho \in [0, r[, s \in [0, L], \theta \in [0, 2\pi]\} \tag{4}$$

A representation of the above definitions is shown in Fig. 1.

**Definition 4** A tubular neighbourhood of a curve $\gamma$ presents *interpenetration of matter* if and only if there exist at least two distinct triples $x$ and $y$ in $\Omega$ with $p(x) = p(y)$ and at least one of the two points belongs to $\text{int}\, T_r$.

**Definition 5** A tubular neighbourhood of a curve $\gamma$ presents *self-contact* if and only if there exist two distinct triples $x$ and $y$ in $\Omega$ with $p(x) = p(y)$ and $p(x), p(y) \in \text{bd}\, T_r$.

***Remark 1*** The boundary of the tubular neighbourhood is not in general the physical boundary of the object: this is true when there is no interpenetration. Indeed, when interpenetration occurs, the physical boundary is only a subset of the boundary of the tubular neighbourhood, because some parts of the boundary are contained into $\text{int}\, T_r$.

We recall now some known properties of tubular neighbourhoods.

**Proposition 1** *If $\gamma$ is a curve of class $C^1$, then for every $r \geq 0$, $T_r[\gamma]$ is the union, as $s$ ranges in $[0, L]$, of the closed spheres $B(\gamma(s), r)$ with centres $\gamma(s)$ and radius $r$ and also the union of all the sections $\Gamma_r(s)$ obtained by intersecting $B(\gamma(s), r)$ with the normal plane to $\gamma$ at $\gamma(s)$. If $\gamma$ has no singularities and $k = \max_{[0,L]} \kappa(s) < +\infty$ is the maximum curvature of $\gamma$, then there exists $r > 0$ with $rk < 1$ such that the boundary $\partial T_r[\gamma]$ of $T_r[\gamma]$ is the disjoint union of the boundaries $\partial\Gamma_r(s)$ of $\Gamma_r(s)$. In this case $\partial T_r[\gamma]$ is at least of class $C^1$, so it admits a tangent plane at every point. Conversely, if there exists $s \in [0, L]$ such that $r\kappa(s) > 1$, then there exists $x \in \operatorname{int}\Omega$ and an open ball centred at $x$ such that $\det \nabla p(x) < 0$ in that ball.*

The last part of the Proposition is developed in Schuricht (2002).
The situation where $r\kappa(s) > 1$ will be called *local interpenetration of matter*, that we want to avoid, so the configurations with $r\kappa(s) > 1$ for some $s$ are considered not physically admissible. Clearly, it is an interpenetration of matter in the sense of Definition 4, but not the only possible one. Here, the superposition of points is due to excessive bending and the points are in some sense near (that is, if the bending were a process, then there would be arbitrarily near points which were not superimposed before the critical bending and superimposed after it). We are more interested to rule out points far away on the boundary but which do come in superposition.
If $T_r$ does not present interpenetration of matter, then $p$ is injective (this is sometimes called global injectivity, to distinguish it from the local conservation of orientation $\det \nabla p(x) > 0$). We remark here that many conditions and formulations were studied to express the global injectivity of $p$, see Lonati and Marzocchi (2024) for details: while many conditions involve local expressions, i.e. local radius of curvature, or geometric characteristics expressed using the arc-length $s$ (Chamekh et al. 2009; Mlika 2018; Chamekh et al. 2020), some of them define global formulations on the object, as for example (Ciarlet and Nečas 1987; Gonzalez et al. 2002; Schuricht 2002).
The next result can be quite easily proved by continuity arguments.

**Theorem 1** *Suppose $H : \mathbb{E}^3 \times [0, 1] \to \mathbb{E}^3$ is a map that deforms continuously the points of a curve $\gamma$ as in Definition 1 and let $H$ be such that $H(\gamma, 0)$ and $H(\gamma, 1)$ belong to different ambient isotopy classes. Suppose moreover that $T_r[\gamma]$ verifies at every $t$ the conditions of Proposition 1 so that the tubular neighbourhood of $H(\gamma, t)$ of radius $r$ has always a regular boundary and it never has local interpenetration of matter. Then there exists $t^* \in ]0, 1[$ such that there is self-contact on $\operatorname{bd} T_r[H(\gamma, t^*)]$ but not for $t < t^*$. Furthermore, there exists $\tau \in ]0, 1[$, $\tau > t^*$, such that $T_r[H(\gamma, \tau)]$ has interpenetration of matter, and this does not happen for $t < t^*$.*

Intuitively, if the midline $H(\gamma, t)$ has to change ambient isotopy class, then it must intersect itself somewhere, but then its tubular neighbourhood must come into contact before that time, and then $t^*$ is just the first time this happens. Obviously, shortly before $H(\gamma, t)$ becomes singular but after a first self-contact, its tubular neighbourhood must have a region of superposition.

**Corollary 1** *A mapping $p$, that describes a neighbourhood with interpenetration of matter, is not injective on the set $\operatorname{bd} T_r$, i.e. there is at least one point of self-contact on $\operatorname{bd} T_r$.*

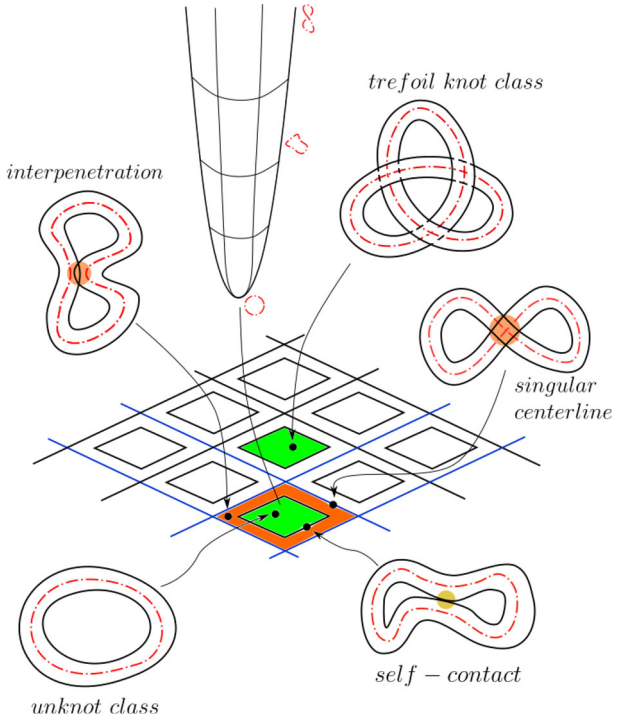


**Fig. 2** Representation of the desired subdivision: every tubular neighbourhood is identified with its centreline $\gamma$. The space of the possible knot types of $\gamma$ is partitioned into isotopy classes, separated by walls (blue lines) that represent configurations with singular knots as centrelines. Each class is divided into two regions: the green one, with physically admissible neighbourhoods and the orange one, with interpenetration of matter. The black squares represent the configurations with self-contact on the boundary and without interpenetration, so physically consistent. We show an example for each mentioned case in the class of the unknot, and an example of the trefoil knot. The paraboloid represents the ideal behaviour of the energy functional that we are looking for, analogous to the one proposed by O'Hara for knots, with a minimum in each prime knot class and the circular centreline as global minimizer

These results allow us to use the same approach of O'Hara: given the radius $r$ of the neighbourhood, we partition the space of configurations of tubular neighbourhoods into cells defined by the knot type of the centreline; we would like to separate these cells with walls of infinite energy, that consist of configurations in which the centreline is a singular knot; moreover, we would like to partition each cell into two regions: one region contains the centrelines that generate tubular neighbourhoods without interpenetration of matter, while the other region contains all the tubular neighbourhoods where interpenetration of matter occurs. Thanks to the previous results, the boundary between the two regions is then characterized by the presence of self-contact points on the boundary of the neighbourhood, but without interpenetration of matter. An intuitive representation of our ideal partition is presented in Fig. 2.
We then need an energy functional that is infinite when there is self-contact or interpenetration of matter and is finite otherwise.

## 3 Geometrical Setting of the Problem

**Definition 6** Given the map $p$ defined by (2), we call the set $\mathcal{A}(s) = \mathrm{Im}(p(\cdot, s, \cdot))$ *cross-section* at $s$, the curve $M(s)(\cdot) = p(r, s, \cdot)$ *meridian* at $s$, and the curve $P(\theta)(\cdot) = p(r, \cdot, \theta)$ *parallel* at angle $\theta$.

By (2), then

$$\begin{aligned} M(s)(\theta) &= \gamma(s) + r\cos\theta \boldsymbol{n}(s) + r\sin\theta \boldsymbol{b}(s), \theta \in [0, 2\pi] \\ P(\theta)(s) &= \gamma(s) + r\cos\theta \boldsymbol{n}(s) + r\sin\theta \boldsymbol{b}(s), s \in [0, L] \end{aligned} \tag{5}$$

We remark that parallels and meridians are closed curves. In our case, having chosen a circular neighbourhood, the meridian is always a circle of radius $r$ with centre at $\gamma(s)$ and lies in a plane perpendicular to $\boldsymbol{t}(s)$, $\forall s \in [0, L]$. Given two points $A(s, \theta)$ and $B(s, \varphi)$ belonging to the same meridian $M(s)$, we denote by $l_{M(s)}(A, B)$ their minimal distance along the meridian. We have immediately

$$\begin{aligned} l_{M(s)}(A, B) :&= \begin{cases} r|\theta - \varphi| & \text{if } |\theta - \varphi| \le \pi \\ r(||\theta - \varphi| - 2\pi|) & \text{if } \pi < |\theta - \varphi| \le 2\pi \end{cases} \\ &= r(2h\pi + (-1)^h|\theta - \varphi|), \quad h = 0, 1, \ |\theta - \varphi| \in [h\pi, (h+1)\pi]. \end{aligned} \tag{6}$$

This is a positive and continuous function on $[0, 2\pi] \times [0, 2\pi]$. Moreover, chosen two points $C(t, \theta)$ and $D(t, \varphi)$, we have $l_{M(s)}(A, B) = l_{M(t)}(C, D)$ for every $s, t \in [0, L]$ because the two couples determine the same arc of circle on bd $T_r$.
Similarly, given two points $A(s_1, \theta)$ and $B(s_2, \theta)$ belonging to the same parallel $P(\theta)$, we denote by $l_{P(\theta)}(A, B)$ their minimal distance along the parallel. Differentiating with respect to $s$ the expression of the parallel in (5), we get

$$\begin{aligned} \hat{l}_\theta(s_1, s_2) &:= \int_{s_1}^{s_2} \left\| \frac{\mathrm{d}}{\mathrm{d}s} P(\theta)(s) \right\| \mathrm{d}s \\ &= \int_{s_1}^{s_2} \sqrt{(1 - r\cos\theta\kappa(s))^2 + r^2\tau(s)^2}\, \mathrm{d}s \end{aligned} \tag{7}$$

where $s$ does not cross $L$. Then, assuming $0 \le s \le t \le L$, denoting with $\tilde{L}_\theta$ the length of $P(\theta)$,

$$\begin{aligned} l_{P(\theta)}(A, B) &= \begin{cases} \hat{l}_\theta(s, t) & \text{if } \hat{l}_\theta(s, t) \le \tilde{L}_\theta/2 \\ \tilde{L}_\theta - \hat{l}_\theta(s, t) & \text{if } \tilde{L}_\theta/2 < \hat{l}_\theta(s, t) \le \tilde{L}_\theta \end{cases} \\ &= h\tilde{L}_\theta + (-1)^h \hat{l}_\theta(s, t) \quad h = 0, 1, \ \hat{l}_\theta(s, t) \in \left[ h\tilde{L}_\theta, (h+1)\frac{\tilde{L}_\theta}{2} \right]. \end{aligned} \tag{8}$$

This is a positive and continuous function of $s$ and $t$ on $[0, L] \times [0, L]$: indeed, it is the smallest length between the one obtained in clockwise direction and the

counterclockwise one. From (7) we have that

$$\left\| \frac{\mathrm{d}}{\mathrm{d}s} P(\theta)(s) \right\|^2 = (1 - r\cos\theta\kappa(s))^2 + r^2\tau(s)^2. \tag{9}$$

While the first term of the right-hand side in (9) is due to the distance along the parallel on bd $T_r$ corresponding to the angle $\theta$ and projected along the vector $\boldsymbol{t}(s)$, we notice that the second term on the right-hand side, i.e. $r^2\tau(s)^2$, originates from a component of $\frac{\mathrm{d}}{\mathrm{d}s} P(\theta)(s)$ orthogonal to the previous one and it comes from the fact that the curve $\gamma$ leaves its osculating plane: indeed, for plane curves, this term vanishes. Anyway, although this contribution is measured along meridians, it has no relationship with the distance $l_{M(s)}$, which has to be added in order to compute a sort of distance between generic points on bd $T_r$. In view of this, we introduce the two finite lengths

$$\begin{aligned} l^{\boldsymbol{t}}_{P(\theta)} &= \int_s^t \left\| \frac{\mathrm{d}}{\mathrm{d}\xi} P(\theta)(\xi) \cdot \boldsymbol{t}(\xi) \right\| \mathrm{d}\xi \\ &= \int_s^t |1 - r\cos\theta\kappa(\xi)| \, \mathrm{d}\xi \\ &= \int_s^t |1 - r\cos\theta(\boldsymbol{n}(\xi) \cdot \boldsymbol{t}'(\xi))| \, \mathrm{d}\xi \end{aligned} \tag{10}$$

i.e. the increment of the length of the parallel between the cross-sections $\mathcal{A}(s)$ and $\mathcal{A}(t)$ projected on the vector $\boldsymbol{t}(\xi)$, $\xi \in [s, t]$, and

$$\begin{aligned} l^{\boldsymbol{n},\boldsymbol{b}}_{P} &= \int_s^t \left\| \frac{\mathrm{d}}{\mathrm{d}\xi} P(\theta)(\xi) \times \boldsymbol{t}(\xi) \right\| \mathrm{d}\xi \\ &= \int_s^t || - \tau(\xi) r \sin\theta \boldsymbol{n}(\xi) + \tau(\xi) r \cos\theta \boldsymbol{b}(s)|| \, \mathrm{d}\xi \\ &= r \int_s^t |\tau(\xi)| \, \mathrm{d}\xi = r \int_s^t |\boldsymbol{n}(\xi) \cdot \boldsymbol{b}'(\xi)| \, \mathrm{d}\xi \end{aligned} \tag{11}$$

i.e. the increment of the length of the parallel projected on the boundary of $\mathcal{A}(\xi)$.
We remark that there is no specification on the angle and in the computation $\theta$ can be any angle, because this contribution does not depend on the parallel taken into consideration. Although $l^2_{P(\theta)} \neq (l^{\boldsymbol{t}}_{P(\theta)})^2 + (l^{\boldsymbol{n},\boldsymbol{b}}_{P})^2$, this relationship is true "infinitesimally" and will help us to define the main functional (see Fig. 3 for the simple case of the helix).

## 4 Definition of the Functional

We recall the Möbius energy functional introduced by O'Hara (1991) for a knot $K$ described by a $C^2$ curve $\gamma$ with fixed length $L$, where $X$ and $Y$ are two points on the knot, whose position is described by their curvilinear abscissas in $[0, L]$. The

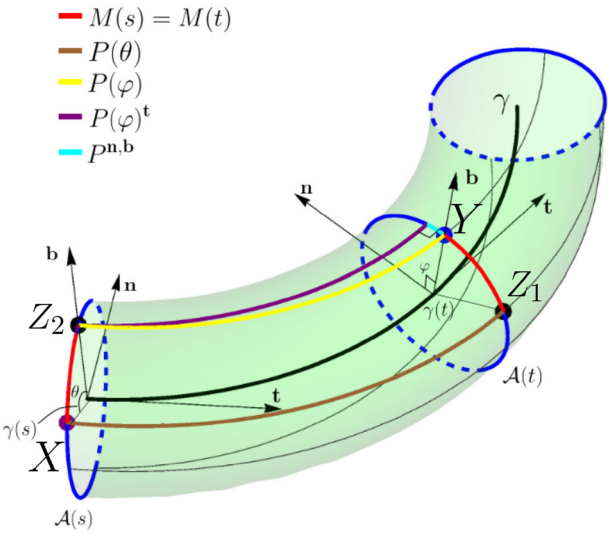


**Fig. 3** As an example, we plot an arc of helix described as the curve $\gamma$, with $\gamma(\xi) = (R\cos(\xi/\lambda), R\sin(\xi/\lambda), a\xi/\lambda), \xi \in [0, 7/2], R = 2, a = 0.5, \lambda = \sqrt{R^2 + a^2}$. We show the tubular neighbourhood $T_r$ around $\gamma$ with radius $r = 0.5$, and we highlight the cross-sections corresponding to $s$ and $t$ and the Serret–Frenet frame in $\gamma(s)$ and $\gamma(t)$, with $s = 0$ and $t = 2$. For the points $X(0, 5\pi/6)$ and $Y(2, \pi/2)$, we have $Z_1(2, 5\pi/6)$, $Z_2(0, \pi/2)$ in the figure. We have the constant curvature $\kappa = R/\lambda^2 \sim 0.47$ and the torsion $\tau = a/\lambda^2 \sim 0.118$. In red, the two arcs of meridians and in yellow and brown the two parallels $P(\theta)$ and $P(\varphi)$. Finally, we show the decomposition of $P(\varphi)$ in a light blue arc $P^{\boldsymbol{n},\boldsymbol{b}}$ on the boundary of $\mathcal{A}(t)$ that has length $\hat{l}_P^{\boldsymbol{n},\boldsymbol{b}} = r\tau(t - s)$ and a purple curve $P(\varphi)^{\mathbf{t}}$ orthogonal to the cross-section $\mathcal{A}(t)$ with length $|t - s - r(t - s)\cos\varphi\kappa|$ that in our case equals $t - s$ because $\varphi = \pi/2$

functional is

$$\begin{aligned}\mathcal{E}(K) &= \int_K \int_K \left(\frac{1}{|X - Y|^2} - \frac{1}{d^2(X, Y)}\right) \mathrm{d}X\,\mathrm{d}Y \\ &= \int_0^L \int_0^L \left(\frac{1}{|\gamma(s) - \gamma(t)|^2} - \frac{1}{\min\{|s - t|, L - |s - t|\}^2}\right) \mathrm{d}s\,\mathrm{d}t\end{aligned} \tag{12}$$

and the integration is performed on the cartesian product between the knot and itself, where $d(X, Y)$ is simply the distance along the knot between the two points, i.e. the difference between their abscissas.

We want to define a similar repulsive energy on a tubular neighbourhood in $\mathbb{E}^3$. We remark, however, that the exponent chosen for the distance between two charges in the electrostatic potential is $-2$, instead of the $-1$ of the Coulomb law. We first choose this exponent following O'Hara's approach, but a more detailed discussion about it will be carried out below.

As was done for the Möbius energy, the main ingredient to distinguish different configurations is to make a comparison between the Euclidean distance between two points $X$ and $Y$ and an expression $d(X, Y)$ that takes into account the geometry of the

configuration. In this way, when two generic points occupy different positions in $\mathbb{E}^3$ the functional is well-defined. Otherwise, the interesting cases are the following:

a) $X = \gamma(s) = \gamma(t) = Y$ with $s = t$, i.e. $X, Y$ occupy the same position in space and they are determined by the same abscissa: then, as $X \to Y$, $|X - Y|$ and $d(X, Y)$ go to zero and the difference between their squared reciprocals may be finite or infinite (of course, one should have a finite limit for the integral and this actually happens for the above distance $|s - t|$ in (12));
b) $X = \gamma(s) = \gamma(t) = Y$ with $s \neq t$, i.e. $X, Y$ occupy the same position in space but come from different points on the abstract knot: then, the second fraction of the integrand is bounded, while the first term diverges to $+\infty$ and so does the energy: it is the case of a singular knot.

Minimizing the integral, b) is avoided, provided the integral is convergent in case a).

We now want to generalize the previous functional to tubular neighbourhoods distinguishing isotopy classes and tubes with or without interpenetration of matter. Therefore, it is natural to use as a fact of distinction between these classes the presence of self-contact between points on the boundary of the tube.
This choice is also motivated by the fact that, for the electrostatic inspiration of this energy, when we imagine our elastic material as a conductor charged in electrostatic equilibrium, the charge distributes on the external surface of the conductor and, being the charge homogeneous, the object presents a repulsive character with itself.
Given two points $X(s, \theta)$ and $Y(t, \varphi)$ on $\mathrm{bd}\, T_r$, we denote

$$Z_1(t, \theta) = P(\theta) \cap M(t), \quad Z_2(s, \varphi) = P(\varphi) \cap M(s) \tag{13}$$

i.e. the point belonging to the same meridian of $Y$ and the same parallel of $X$ and the point belonging to the same meridian of $X$ and the same parallel of $Y$, respectively. Next, we set $\hat{l}_{P(\theta)}$ to be the length of the parallel $P(\theta)$ between $X$ and $Z_1$ as in (8), that will be decomposed into two components as before and analogously with the length $\hat{l}_{P(\varphi)}$ of the parallel $P(\varphi)$ between $Y$ and $Z_2$. Finally, by $l_{M(s)}$ we denote the length of the meridian corresponding to $s$ between $X$ and $Z_2$ and by $l_{M(t)}$ we denote the length of the meridian corresponding to $t$ between $Y$ and $Z_1$ as in (6). In particular, $l_{M(s)} = l_{M(t)}$, then we denote it with $l_M$.

**Definition 7** Given a curve $\gamma$ of class $C^3$ and a tubular neighbourhood $T_r[\gamma]$ around $\gamma$ with radius $r > 0$, we define

$$\begin{aligned} F(T_r) &= \int\limits_{\mathrm{bd}\, T_r \times \mathrm{bd}\, T_r} \left( \frac{1}{|X - Y|^2} - \frac{1}{d^{*2}(X, Y)} \right) \mathrm{d}S\, \mathrm{d}S \\ &= \int_0^L \int_0^L \int_0^{2\pi} \int_0^{2\pi} \left( \frac{1}{|p(r, s, \theta) - p(r, t, \varphi)|^2} \right. \\ &\quad \left. - \frac{1}{d^{*2}(p(r, s, \theta), p(r, t, \varphi))} \right) \mathrm{d}\varphi\, \mathrm{d}\theta\, \mathrm{d}t\, \mathrm{d}s \end{aligned} \tag{14}$$

where $|X - Y|$ is the Euclidean distance

$$|X(s,\theta) - Y(t,\varphi)| = |\gamma(s) - \gamma(t) + r(\cos\theta \boldsymbol{n}(s) - \cos\varphi \boldsymbol{n}(t)) + r(\sin\theta \boldsymbol{b}(s) - \sin\varphi \boldsymbol{b}(t))| \tag{15}$$

and $d^{*2}(X, Y)$ is, assuming $s < t$ for simplicity,

$$d^{*2}(X(s,\theta), Y(t,\varphi)) = (l_M + \hat{l}_P^{\boldsymbol{n},\boldsymbol{b}})^2 + \hat{l}^{\boldsymbol{t}}_{P(\theta)} \hat{l}^{\boldsymbol{t}}_{P(\varphi)} \tag{16}$$

where the quantities are defined in (6), (10), (11).

In words, we sum the projection of the parallel on the cross-section with the arc of meridian, so the first part is an arc on the boundary of the cross-section, while the second part is made up of two curves orthogonal to $\mathcal{A}(\xi)$, $\forall \xi \in [s, t]$.

***Remark 2*** If the midline $\gamma$ lies in a plane, then $d^{*2}(X, Y)$ reduces to $\hat{l}_{P(\theta)}\hat{l}_{P(\varphi)} + l_{M(s)}l_{M(t)} = \hat{l}_{P(\theta)}\hat{l}_{P(\varphi)} + l_M^2$, where $\hat{l}_P$ is defined in (8), since the torsion vanishes, and the parallels are plane curves.

***Remark 3*** $d^{*2}(X, Y)$ is a positive quantity which vanishes if and only if $X \equiv Y$ and is a symmetric function of $X$ and $Y$. However, $d^*$ is not a distance on bd $T_r$ because it does not satisfy the triangle inequality. As a counterexample, one may take $X = (R - r, 0, 0)$, $Y = (0, R, r)$, $Z = \left(\left(R - r\cos\frac{\pi}{6}\right)\cos\frac{\pi}{3}, \left(R - r\cos\frac{\pi}{6}\right)\sin\frac{\pi}{3}, r\sin\frac{\pi}{6}\right)$, that lie on the boundary of a torus, and verify directly that

$$\begin{aligned} d^{*2}(X, Y) &\geq d^{*2}(X, Z) + d^{*2}(Z, Y) + 2\sqrt{d^{*2}(X, Z)}\sqrt{d^{*2}(Z, Y)} \\ &= (d^*(X, Z) + d^*(Z, Y))^2. \end{aligned}$$

***Remark 4*** An intuitive expression for playing the role of $d(X, Y)$ in our model would be the shortest distance on bd $T_r$ between $X$ and $Y$, i.e. the length of the shortest geodesic on the surface between the two points. However, the difficulty in its explicit calculation is prohibitive for specific results on a generic configuration.

## 5 Main Results

We now prove the main results on our functional. Similarly to the knot energy (12), we can prove that it is bounded on a torus with circular centreline (instead that on a circular knot), that diverges only when two points on the boundary are different on the object (have different coordinates) but coincide in the space, that is bounded and continuous in the topology of the space of functions to which $\gamma$ belongs. The analogous results were proved in O'Hara (1991) for Möbius energy.

***Remark 5*** In order to define the functional $F(T_r)$ as invariant under a reparametrization of $\gamma$, as was done for Möbius energy, it is sufficient to multiply the integrand of the functional by $|\gamma'(s)||\gamma'(t)|$, where in general it could be $|\gamma'| \neq 1$.

**Theorem 2** *The functional $F(T_r)$ is positive, has finite value and is bounded from below on a tubular neighbourhood of a circular centreline, i.e. a torus, that does not present interpenetration of matter in its interior or self-contact on its boundary.*

***Proof*** Let $R$ be the radius of the centreline of the torus in the plane $z = 0$ and $r$ the radius of its generating circle; we assume $R > r$ to avoid interpenetration of matter or self-contact and we reparametrize the midline so that the new parameters $u, v$ vary from 0 to $2\pi$. We start proving that the functional is bounded from above.
We consider two generic points $X, Y$ on bd $T_r$ with latitudes $\theta, \varphi$ and longitudes $u, v$. Setting

$$a = R - r\cos\theta,\ \ b = R - r\cos\varphi,$$

we have $a, b > 0$ since $R > r$ and then

$$X = (a\cos u, a\sin u, r\sin\theta), \quad Y = (b\cos v, b\sin v, r\sin\varphi).$$

Moreover, setting $c = r(\sin\theta - \sin\varphi)$, the euclidean distance between $X$ and $Y$ is easily found as

$$|X - Y|^2 = a^2 + b^2 + c^2 - 2ab\cos(v - u).$$

From (16), $d^{*2}(X, Y)$ is given by $r^2|\theta - \varphi|^2 + ab|v - u|^2$, if $|\theta - \varphi| \le \pi$ and $|v - u| \le \pi$ and

$$r^2(2h\pi + (-1)^h|\theta - \varphi|)^2 + ab(2k\pi + (-1)^k|v - u|)^2$$

in the other cases, for $h, k = 0, 1$, $|\theta - \varphi| \in [h\pi, (h+1)\pi]$, $|v - u| \in [k\pi, (k+1)\pi]$. We perform the integration in the first case; the others are similar. Set $x = v - u$ and $y = \theta - \varphi$ and suppose $v > u$ and $\theta > \varphi$ by symmetry, so that

$$\begin{aligned} F(T_r) &= \int_{[0,2\pi]^4}\left(\frac{1}{|X - Y|^2} - \frac{1}{d^{*2}(X, Y)}\right)\mathrm{d}v\,\mathrm{d}u\,\mathrm{d}\varphi\,\mathrm{d}\theta \\ &= 4\int_0^{2\pi}\int_0^{\pi}\int_0^{2\pi}\int_0^{\pi}\left(\frac{1}{|X - Y|^2} - \frac{1}{d^{*2}(X, Y)}\right)\mathrm{d}x\,\mathrm{d}u\,\mathrm{d}y\,\mathrm{d}\varphi \\ &= 8\pi\int_0^{2\pi}\int_0^{\pi}\int_0^{\pi}\left(\frac{1}{|X - Y|^2} - \frac{1}{d^{*2}(X, Y)}\right)\mathrm{d}x\,\mathrm{d}y\,\mathrm{d}\varphi. \end{aligned}$$

Now we carry out the first integration and show that the function obtained has finite values on the domain $[0, 2\pi] \times [0, 2\pi]$, with $|\theta - \varphi| \leq \pi$.
First, we have

$$\int_0^\pi \frac{1}{|X-Y|^2}\,dx = \int_0^\pi \frac{1}{a^2+b^2+c^2-2ab\cos x}\,\mathrm{d}x = \frac{\pi}{\sqrt{((a-b)^2+c^2)((a+b)^2+c^2)}}$$

Since $a = R - r\cos(\varphi + y), b > 0$, this integral is infinite if and only if $a = b$ and $c = 0$ that is equivalent to $y = 0$, i.e. $\theta = \varphi$. Otherwise, we have

$$\int_0^\pi \frac{1}{d^{*2}(X,Y)}\,\mathrm{d}x = \int_0^\pi \frac{1}{r^2y^2+abx^2}\,\mathrm{d}x = \frac{1}{ry\sqrt{ab}}\arctan\left(\frac{\sqrt{ab}\pi}{ry}\right), \quad (y \neq 0).$$

So, for $y \neq 0$ both integrals have finite values and so the functional has finite value because in the next integrations $\theta, \varphi$ are bounded. Then we analyse the limit of the integrand when $y \to 0$, i.e. $\varphi \to \theta$. For $\varphi \to \theta$ we have $a \to b > 0$, and using the expansion

$$\arctan\left(\frac{\sqrt{ab}\pi}{ry}\right) \sim \frac{\pi}{2} - \frac{ry}{\sqrt{ab}\pi}$$

the limit becomes, after some calculations using half-angle and prosthaphaeresis formulae,

$$\lim_{y\to 0}\left(\frac{\pi}{4r\left|\sin\left(\frac{y}{2}\right)\right|}\cdot \frac{1}{\sqrt{\left(R - r\cos\left(\varphi+\frac{y}{2}\right)\left(\cos\left(\frac{y}{2}\right)\right)\right)^2 + r^2\left(\cos\left(\varphi+\frac{y}{2}\right)\sin\left(\frac{y}{2}\right)\right)^2}} - \frac{\pi}{2r|y|\sqrt{ab}} + \frac{1}{\pi ab}\right) = \frac{1}{\pi a^2} < +\infty. \tag{17}$$

Indeed, we notice in particular that the part containing $y$ is infinitesimal since

$$\frac{1}{\sin y} - \frac{1}{y} \sim \frac{y}{6}, \quad (y \to 0)$$

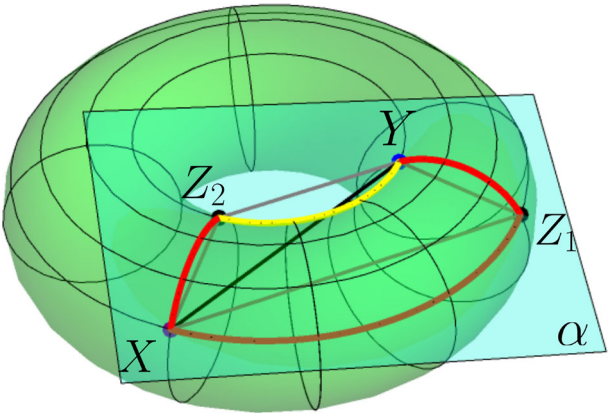


**Fig. 4** The torus with the four points $X, Y, Z_1, Z_2$ with the parameters $R = 2, r = 1, u = \frac{11\pi}{6}, v = \frac{\pi}{3}, \theta = \frac{\pi}{3}, \varphi = \frac{5\pi}{6}$. In red the two arcs of meridians considered in $d^{*2}$, in yellow the parallel at angle $\varphi$ and in brown the parallel at angle $\theta$. The four points belong to the same plane $\alpha : 1.43x + 0.38y + 3.92z - 4.96 = 0$ plotted in light blue

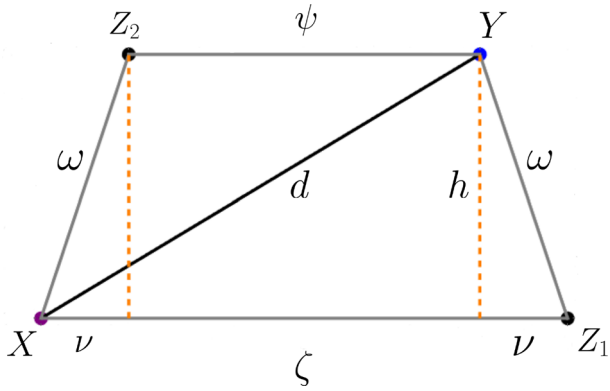


**Fig. 5** The construction of the isosceles trapezoid in the plane $\alpha$; we use Pythagoras' theorem to find an equality involving the two bases $\zeta$ and $\psi$, the edges $\omega$ and the diagonal $d$

and this shows that the preceding limit is finite and that the squared Euclidean distance and $d^{*2}$ degenerate at the same order when $X \to Y$, so the two divergences compensate.

We prove that the functional is bounded from below. Taken any two points $X$ and $Y$ on bd $T_r$ and taken $Z_1$ and $Z_2$ as in (13), we know that all the parallels on a torus are planar circular arcs, that lie in planes parallel to the plane $z = 0$ of the centreline, while the meridians are all congruent circles. As shown in Fig. 5, we consider the segments $XZ_1$ with length $\zeta$, $YZ_2$ with length $\psi$, that have in general different lengths and the congruent segments $XZ_2$ and $YZ_1$ with length $\omega$, while we denote with $\overline{XY} = d$ the length of the segment that connects $X$ and $Y$.

As shown in Fig. 4, the four points all lie on a plane $\alpha$, and thus they define a planar polygon with four edges. Indeed, simple calculations show immediately that

$$\det\begin{pmatrix} XZ_2 \\ XZ_1 \\ XY \end{pmatrix} = \det\begin{vmatrix} r\cos u(\cos\varphi - \cos\theta) & r\sin u(\cos\varphi - \cos\theta) & \omega \\ \zeta(\cos u - \cos v) & \zeta(\sin u - \sin v) & 0 \\ \zeta\cos u - \psi\cos v & \zeta\sin u - \psi\sin v & \omega \end{vmatrix} = 0$$

i.e. the four points lie on the same plane.
Moreover, $YZ_2 = (\psi(\cos u - \cos v), \psi(\sin u - \sin v), 0)$, that is clearly parallel to $XZ_1$ and this implies that the quadrilateral defined in the plane $\alpha$ is an isosceles trapezoid. Now, from a standard reasoning, using Pythagoras' Theorem and calling $\nu = (\zeta - \psi)/2$ and $h$ the height, we have

$$\begin{aligned} |X - Y|^2 = d^2 &= h^2 + (\zeta - \nu)^2 \\ &= \omega^2 - \nu^2 + \zeta^2 + \nu^2 - 2\zeta\nu = \omega^2 + \zeta\psi \\ &= (XZ_2)^2 + XZ_1 \cdot YZ_2 \end{aligned}$$

Now, it is obvious that the segment $XZ_2$ is shorter than the shortest arc of meridian connecting $X$ and $Z_2$ (and the same for $Y$ and $Z_1$) and that $XZ_1$ and $YZ_2$ are shorter than the minimal arc of parallel connecting the points (red, yellow and brown arcs in Fig. 4), so it is true that

$$|X - Y|^2 \le l_M^2 + \hat{l}_{P(\theta)}\hat{l}_{P(\varphi)}$$

and thanks to Remark 2 the second term is exactly $d^{*2}(X, Y)$.
Then $d^{*2}(X, Y) \ge |X - Y|^2$, and

$$\frac{1}{|X - Y|^2} \ge \frac{1}{d^{*2}(X, Y)}$$

and the integrand is greater or equal to 0 and is integrated on bounded intervals; this implies that the functional is positive and thus bounded from below. □

***Remark 6*** We have that $d^{*2}(X, Y) = 0$ holds iff $s = t$ and $\theta = \varphi$, i.e. $X = Y$.
While one implication is trivial, if $d^{*2}(X, Y)$ vanishes, then, being the sum of positive quantities, both must vanish, so $l_M = 0$ implies $\theta = \varphi$ and

$$\int_s^t r|\tau(\xi)|\,\mathrm{d}\xi = 0$$

which implies either $t = s$, i.e. $X = Y$, or $\tau(\xi) = 0$ for every $\xi$, but then the arc of centreline is a plane curve. Now from $\hat{l}_{P(\theta)}\hat{l}_{P(\varphi)} = 0$ and $s \ne t$ it follows that two cases can hold: $1 - r\cos\theta\kappa(\xi) = 0$ for all $\xi$ as above, or $1 - r\cos\varphi\kappa(\xi) = 0$. But then in both of them $\kappa$ is constant and therefore the above arc is a circumference with radius $\rho = r\cos\theta$ and $\kappa\rho = 1$, which implies local interpenetration. Therefore it must be $s = t$ and thus $X = Y$.

We now prove some results for a general regular closed midline.

**Theorem 3** *The functional $F(T_r) > -\infty$, for any $T_r[\gamma]$ with $\gamma \in C^3([0, L], \mathbb{R}^3)$.*

***Proof*** Since integration is on bounded intervals, the boundedness of the integrand is sufficient. The integrand is given by the difference of two positive quantities, so it can degenerate to $-\infty$ only if the denominator of the second term goes to 0 while the denominator of the first one is bounded away from zero or it converges to 0 with a different order. From the previous Remark, $d^{*2}$ tends to 0 iff $X \to Y$ on the rod, i.e. $s \to t$ and $\theta \to \varphi$, then also $|X - Y| \to 0$. Both fractions diverge and we have to carefully study the behaviour of the integrand.
We can assume $X(s, \theta)$, $Y(t, \varphi)$, with $t = s + \eta_1$ and $\varphi = \theta + \eta_2$ where $\eta_i$ are respectively a small displacement along the centreline and a small variation in the angle on the cross-section. We also assume a positive torsion; with a negative torsion of $\gamma$ the proof is analogous. We expand the expression of $|X - Y|$ using the above notation for $t$ and $\varphi$: in particular we expand $\gamma(t)$, $\boldsymbol{n}(t)$ and $\boldsymbol{b}(t)$ with Taylor series up to the third order in $\eta_1$ and $\cos\varphi$ and $\sin\varphi$ with Taylor series up to the fourth order in $\eta_2$. We then proceed by collecting the terms of the components along $\boldsymbol{t}(s)$, $\boldsymbol{n}(s)$ and $\boldsymbol{b}(s)$. From orthogonality of the Serret–Frenet frame, we compute the standard squared norm of $X - Y$, obtaining, through long but easy computations through the software Mathematica (Wolfram Inc., version 13)

$$|X - Y|^2 = |p(r, s, \theta) - p(r, s + \eta_1, \theta + \eta_2)|^2 = A_2 + A_3 + A_4 + o_5(\eta_1, \eta_2)$$

where $A_k$ denote the terms of $k$th degree in $\eta_1$, $\eta_2$ and $o_5$ is at least of fifth degree in $\eta_1$, $\eta_2$. We notice that

$$\begin{aligned} A_2 &= \eta_1^2 + r^2\cos^2\theta\eta_1^2\kappa(s)^2 - 2\eta_1^2 r\cos\theta\kappa(s) + r^2\eta_2^2 \\ &\quad + r^2\tau(s)^2\eta_1^2 + 2r^2\eta_1\eta_2\tau(s) \\ &= \eta_1^2(1 - r\kappa(s)\cos\theta)^2 + r^2(\eta_2 + \eta_1\tau(s))^2. \end{aligned}$$

The expressions of $A_k$ for $k = 3, 4$ are given in the Appendix. On the other hand, we proceed in the same way with

$$\begin{aligned} d^{*2}(X, Y) = &\int_s^{s+\eta_1} |1 - r\cos\theta\kappa(\xi)|\,\mathrm{d}\xi \int_s^{s+\eta_1} |1 - r\cos(\theta + \eta_2)\kappa(\xi)|\,\mathrm{d}\xi \\ &+ r^2\left(\eta_2 + \int_s^{s+\eta_1} |\tau(\xi)|\,\mathrm{d}\xi\right)^2 \end{aligned}$$

expanding the integrals from $s$ to $s+\eta_1$ with Taylor series up to the third order in $\eta_1$ and $\cos\varphi$ with Taylor series up to the fourth order in $\eta_2$, thus finding using Mathematica

$$d^{*2}(X, Y) = A_2 + A_3 + B_4 + o_5(\eta_1, \eta_2)$$

where $A_k$, $B_k$ denote the terms of $k$th degree in $\eta_1$, $\eta_2$ and $o_5$ is at least of fifth degree in $\eta_1$, $\eta_2$. While $A_2$, $A_3$ coincide with the above ones, $B_4$ is different and its expression

is given in the Appendix. Then, the integrand becomes

$$\frac{1}{A_2 + A_3 + A_4 + o_5(\eta_1, \eta_2)} - \frac{1}{A_2 + A_3 + B_4 + o_5(\eta_1, \eta_2)}$$

which behaves for $\eta_1, \eta_2 \to 0$ as

$$\frac{B_4 - A_4 + o_5}{A_2^2 + o_5}$$

that is the ratio between two poynomials of fourth degree and which can diverge in $(\eta_1, \eta_2) = (0, 0)$ if and only if $A_2$ tends to zero. But it is easily seen that $A_2$ is a positive definite quadratic form if $1 - r\kappa(s)\cos\theta \neq 0$, which means that $r\kappa(s) < 1$ which is true by assumption of local non-interpenetration of matter. Then the integrand is also bounded, since it is bounded when $\eta_1, \eta_2 \to 0$ and elsewhere bounded. □

**Theorem 4** *If non-interpenetration of matter holds, the functional degenerates to* $+\infty$ *if and only if there is at least a self-contact between points belonging to* bd $T_r$.

***Proof*** It is sufficient to consider the case of a single isolated self-contact point, so we assume that there exist $A, B$ in bd $T_r$ such that $|A - B| = 0$, with $(s, \theta) \neq (t, \varphi)$ (that implies $s \neq t$). Without losing in generality we can consider two disjoint thin cylinders with perpendicular axes touching externally; indeed, we have that the segment joining the centres $\gamma(s)$ and $\gamma(t)$ of two cross-sections that are in contact is orthogonal to $\boldsymbol{t}(s)$ and $\boldsymbol{t}(t)$. This fact has been pointed out by many Authors, but it is explained in detail in [Lonati and Marzocchi (2024), pp. 7–8].
Thus, we take $X = (x, r\sin\theta, r - r\cos\theta)$ and $Y = (-r\sin\varphi, y, -r + r\cos\varphi)$, $\theta, \varphi \in [0, 2\pi]$ and $x, y$ belonging to a suitable small interval $[-L, L]$, $L > 0$. Now

$$|X - Y|^2 = (x + r\sin\varphi)^2 + (y - r\sin\theta)^2 + (r(1 - \cos\theta) + r(1 - \cos\varphi))^2$$

Since $X \neq Y$ elsewhere, we consider only

$$I = \int_{-L}^{L}\int_{-L}^{L}\int_{-\pi}^{\pi}\int_{-\pi}^{\pi} \frac{1}{|X - Y|^2}\,\mathrm{d}\varphi\,\mathrm{d}\theta\,\mathrm{d}x\,\mathrm{d}y.$$

Using the inequality $(x \pm y)^2 \leq 2(x^2 + y^2)$, we obtain

$$(x + r\sin\varphi)^2 \leq 2(x^2 + r^2\sin^2\varphi)$$
$$(y - r\sin\theta)^2 \leq 2(y^2 + r^2\sin^2\theta)$$

and

$$(r(1 - \cos\theta) + r(1 - \cos\varphi))^2 \leq 2r^2((1 - \cos\theta)^2 + (1 - \cos\varphi)^2).$$

Replacing into $I$ and using the fundamental trigonometric identity, we get

$$I \geq \frac{1}{2} \int_{-L}^{L} \int_{-L}^{L} \int_{-\pi}^{\pi} \int_{-\pi}^{\pi} \frac{\mathrm{d}x\, \mathrm{d}y\, \mathrm{d}\varphi\, \mathrm{d}\theta}{x^2 + y^2 + r^2(1 - \cos\theta) + r^2(1 - \cos\varphi)}.$$

Since the integrand is positive, integration on $[-L, L]^2$ is greater than on $C = \{(x, y) : x^2 + y^2 \leq L^2\}$. So

$$I \geq \frac{1}{2} \int_C \int_{-\pi}^{\pi} \int_{-\pi}^{\pi} \frac{1}{x^2 + y^2 + r^2 A^2} \,\mathrm{d}\varphi\, \mathrm{d}\theta\, \mathrm{d}x\, \mathrm{d}y =: J,$$

with $A^2 = (1 - \cos\theta) + (1 - \cos\varphi)$. $J$ is easily computed with polar coordinates and it yields

$$J = \frac{\pi}{2} \int_{-\pi}^{\pi} \int_{-\pi}^{\pi} \log\left(1 + \frac{L^2}{r^2 A^2}\right) \mathrm{d}\theta\, \mathrm{d}\varphi$$

and since the length $L$ can be assumed small, using $\log(1 + x^2) \geq \tilde{C}x^2$ for some $\tilde{C} > 0$ and knowing that $1 - \cos x \leq x^2/2$, we get

$$\begin{aligned} I &\geq \frac{\tilde{C}\pi}{2} \frac{L^2}{r^2} \int_{-\pi}^{\pi} \int_{-\pi}^{\pi} \frac{1}{(1 - \cos\theta) + (1 - \cos\varphi)} \,\mathrm{d}\theta\, \mathrm{d}\varphi \\ &\geq \frac{\tilde{C}\pi}{2} \frac{L^2}{r^2} \int_{-\pi}^{\pi} \int_{-\pi}^{\pi} \frac{2}{\theta^2 + \varphi^2} \,\mathrm{d}\theta\, \mathrm{d}\varphi \end{aligned}$$

which is positively divergent.
Viceversa, if the functional is positively divergent, then this must be caused by its first integrand, so $|X - Y| = 0$ and $X$ and $Y$ occupy the same position in space, for some $X$ and $Y$ belonging bd $T_r$. Thus, it may be $d^{*2}(X, Y) = 0$ or $d^{*2}(X, Y) \neq 0$. In the first case, $X(s, \theta)$ and $Y(t, \varphi)$ coincide also in $\Omega$ (i.e. $s = t$ and $\theta = \varphi$) but by Theorem 3, the convergence of the functional is not affected by points on the diagonal of $\Omega \times \Omega$. In the second case $X$ and $Y$ do not coincide in $\Omega$ and we have self-contact. □

By Theorem 4 and Corollary 1, it follows that the functional diverges also for neighbourhoods with interpenetration of matter.

***Remark 7*** By previous results, and having used minimal lengths in the definition of $d^{*2}$, when there is no self-contact the integrand of the functional is continuous on the set of couples $(\theta, \varphi)$, such that $|\theta - \varphi| = \pi$ and on the set of couples $(s, t)$, such that $\int_s^t \sqrt{(1 - r\cos\theta\kappa(u))^2 + r^2\tau(u)^2}\,\mathrm{d}u = \tilde{L}_\theta/2$. We remark that on these set of points, it is not differentiable.

We denote by $\mathbb{T}$ the tubular neighbourhood of a circle $S^1$ in $\mathbb{R}^3$ of length $L$ and we define $\mathcal{L} = \{g : \mathbb{T} \to T_r[\gamma] \subset \mathbb{R}^3$ such that $F(T_r) < +\infty\}$.

**Theorem 5** *The functional $F : \mathcal{L} \to \mathbb{R}$ is continuous with respect to the $C^3$-topology of the centreline $\gamma$.*

***Proof*** We want to prove that small deformations of $\gamma$ produce small variations in the functional. The Euclidean distance and $d^{*2}$ are compositions of continuous functions of $\gamma$ and the Serret–Frenet frame, the curvature and the torsion of $\gamma$, which are continuous with respect to the $C^3$-topology of the centreline $\gamma$.
Then, by the continuity of the function $x \mapsto 1/x, \forall \varepsilon > 0$ there exists a neighbourhood $I \subseteq C^3([0, L], \mathbb{E}^3)$ such that for every $\eta \in I$ and $u = (s, t, \theta, \varphi)$,

$$\left| \frac{1}{|X - Y|^2_\eta(u)} - \frac{1}{|X - Y|^2_\gamma(u)} \right| < \frac{\varepsilon}{8\pi^2 L^2},$$
$$\left| \frac{1}{d^{*2}(X, Y)_\eta(u)} - \frac{1}{d^{*2}(X, Y)_\gamma(u)} \right| < \frac{\varepsilon}{8\pi^2 L^2}$$

whence it follows

$$\left| \left( \frac{1}{|X - Y|^2_\eta(u)} - \frac{1}{d^{*2}(X, Y)_\eta(u)} \right) - \left( \frac{1}{|X - Y|^2_\gamma(u)} - \frac{1}{d^{*2}(X, Y)_\gamma(u)} \right) \right| < \frac{\varepsilon}{4\pi^2 L^2}$$

and integrating, we have $|F(\eta) - F(\gamma)| < \varepsilon$. □

## 6 Möbius Energy as a Particular Case

In Freedman et al. (1994), the Authors proved that Möbius energy presents a minimizer in each prime knot isotopy class, a so-called "optimal knot", and that the circle is the global minimizer between all these classes.
We show now that setting $r = 0$ we obtain the particular case of the O'Hara's energy functional (12) for knots. We remark that we limit our treatment here to simple considerations when $r = 0$, but a further study could include results on a possible $\Gamma$-convergence of our functional to O'Hara's one when $r \to 0$.
If we assume that the radius of the neighbourhood vanishes, we have the following modifications.

1. the tubular neighbourhoods are contracted to knots described by the curve $\gamma$, that can be now taken in $C^2([0, L], \mathbb{R}^3)$ as proposed by O'Hara (1991);
2. the notion of interpenetration of matter loses meaning: indeed, a knot does not have internal points. The space of knots is subdivided into cells, where the region plotted in orange in Fig. 2 does not exist anymore. The boundary of the green region in each cell, i.e. the set of configurations of self-contact of rods coincides with the boundary of the cell itself: it indicates the coincidence between points on the knot, i.e. a singular knot with at least a double point, as in O'Hara's treatment;

3. the functional reduces to (12), i.e. to O'Hara's one; the Euclidean distance between points on bd $T_r$ becomes the Euclidean distance between points on the knot and $d^{*2}$ becomes the squared difference between the curvilinear abscissas that describe the position of $X$ and $Y$. Indeed, substituting $r = 0$ in (6) and (11) we obtain vanishing contributions, while in (10) we obtain a vanishing contribution and $\int_s^t 1 \, \mathrm{d}\xi = t - s$. Thus, from (16), $d^{*2}$ reduces to $(t-s)^2$. Moreover, the angles $\theta$ and $\varphi$ are no more defined.

## 7 Discussion on the Exponent

Many generalizations of Möbius energy were studied in the last three decades, involving in particular the use of a different exponent for the two denominators of the functional or for the integrand, and the minimization of the energy or its coupling with an elastic energy on the knot, see for details (O'Hara 1992, 1994, 2008; Kim and Kusner 1993; Freedman et al. 1994; Buck and Orloff 1995; Simon 1996; Mosel 1998). We carry out here a brief discussion on the possible exponent that can be chosen inside the integrand, recovering the same result obtained for the Möbius energy.
In the definition of the energy we used an exponent 2 for the Euclidean distance, and the same was intuitively done also for $d^*$. We can now study which are the exponents that guarantee divergence of the functional only in presence of a self-contact point: in particular, for O'Hara's energy in (12), as exponent one can choose $\alpha \in [2, 3)$: $\alpha < 3$ provides a compensation of the two divergences in the integrand when $X \to Y$, while $\alpha \geq 2$ assures divergence for a double point.
The same result is valid also for tubular neighbourhoods.

**Theorem 6** *The energy functional*

$$F(T_r) = \int_{\mathrm{bd}^2 T_r} \left( \frac{1}{|X - Y|^\alpha} - \frac{1}{(d^{*2}(X, Y))^{\frac{\alpha}{2}}} \right) \mathrm{d}S \, \mathrm{d}S \tag{18}$$

*is bounded on tubular neighbourhoods without self-contact or interpenetration of matter if* $\alpha \in (0, 3)$, $\alpha \in \mathbb{R}$. *Moreover, the functional diverges for* $T_r$ *if there exists a finite number of self-contact points on* bd $T_r$ *if* $\alpha \geq 2$ *and converges for* $\alpha < 2$. *Finally, if there is a line of self-contact points, (18) diverges also for* $\alpha \in [1, 2)$.

***Proof*** As explained above in Theorem 3, the energy is in general bounded for such objects without self-contact and the unique case that one has to carefully study is when $(t, \varphi) \to (s, \theta)$, i.e. we have to prove that $|X - Y|^\alpha \to 0$ and $d^{*2}(X, Y)^{\alpha/2} \to 0$ with

the same order. We have, using the same notation of the proof of Theorem 3,

$$\begin{aligned} F^{\alpha}(T_r) &= \int_{\mathrm{bd}\, T_r}\int_{\mathrm{bd}\, T_r} \frac{1}{(|X-Y|^2)^{\frac{\alpha}{2}}} - \frac{1}{d^{*2}(X,Y)^{\frac{\alpha}{2}}} \\ &= \int_{\mathrm{bd}\, T_r}\int_{\mathrm{bd}\, T_r} \frac{1}{(A_2+A_3+A_4+o_5(\eta_1,\eta_2)_{|\cdot|})^{\frac{\alpha}{2}}} \\ &\quad - \frac{1}{(A_2+A_3+B_4+o_5(\eta_1,\eta_2)_{d^{*2}}))^{\frac{\alpha}{2}}} \\ &= \int_{\mathrm{bd}^2\, T_r} \frac{(A_2+A_3+B_4+o_5(\eta_1,\eta_2)_{d^{*2}})^{\frac{\alpha}{2}} - (A_2+A_3+A_4+o_5(\eta_1,\eta_2)_{|\cdot|})^{\frac{\alpha}{2}}}{[(A_2+A_3+A_4+o_5(\eta_1,\eta_2)_{|\cdot|})(A_2+A_3+B_4+o_5(\eta_1,\eta_2)_{d^{*2}})]^{\frac{\alpha}{2}}} \end{aligned}$$

We study the integrand in a neighbourhood of $(\eta_1, \eta_2) = (0, 0)$; having all bounded quantities, in both the numerator and the denominator we retain the terms with lower degree: the denominator of the integrand has the smallest degree equal to $4\frac{\alpha}{2} = 2\alpha$. We now study the numerator, denoting $\Phi = A_2 + A_3 + B_4 + o_5(\eta_1, \eta_2)_{d^{*2}}$ and $\Xi = A_2 + A_3 + A_4 + o_5(\eta_1, \eta_2)_{|\cdot|}$, then it has the form $\Phi^{\frac{\alpha}{2}} - \Xi^{\frac{\alpha}{2}}$. We apply the mean value Theorem to the function $f(x) = x^a$ on the closed interval $[\Xi, \Phi]$ (we can assume $\Phi > \Xi$ without losing in generality). This implies that there exists $\Theta \in [\Xi, \Phi]$ such that

$$\frac{f(\Phi) - f(\Xi)}{\Phi - \Xi} = f'(\Theta)$$

i.e. $\Phi^a - \Xi^a = (\Phi - \Xi)a\Theta^{a-1}$ and $A_2 + A_3 + A_4 + o_5(\eta_1, \eta_2)_{|\cdot|} < \Theta < A_2 + A_3 + B_4 + o_5(\eta_1, \eta_2)_{d^{*2}}$. It is sufficient for our study to retain the second degree, then $\Theta$ is of second degree. Moreover, $\Phi - \Xi = B_4 - A_4 + o_5(\eta_1, \eta_2)_{d^{*2}} - o_5(\eta_1, \eta_2)_{|\cdot|}$, so is of fourth degree. Finally, $a = \alpha/2$, then $\Phi^{\alpha/2} - \Xi^{\alpha/2} \sim (\alpha/2)(B_4 - A_4)A_2^{(\alpha/2)-1}$ and finally the numerator is of degree $4 + 2 * ((\alpha/2) - 1) = 2 + \alpha$.

Then, to have a convergent integral we must require $2+\alpha+1 > 2\alpha$, then for $\alpha < 3$ the functional is finite for tubular neighbourhoods without self-contact or interpenetration of matter.

For the proof of the divergence in case of at least a self-contact point with $\alpha \geq 2$, we proceed as in Theorem 4. Suppose there exists an isolated point of self-contact. We study the behaviour of the integral

$$\begin{aligned} I_{\alpha} &= \int_{-L}^{L}\int_{-L}^{L}\int_{-\pi}^{\pi}\int_{-\pi}^{\pi} \frac{1}{|X-Y|^{\alpha}}\, \mathrm{d}\varphi\, \mathrm{d}\theta\, \mathrm{d}x\, \mathrm{d}y \\ &=: \int_{[-L,L]^2\times[-\pi,\pi]^2} \frac{1}{D^{\alpha}}\, \mathrm{d}\varphi\, \mathrm{d}\theta\, \mathrm{d}x\, \mathrm{d}y \end{aligned}$$

Notice first that if $\Omega_L = [-L, L]^2 \times [-\pi, \pi]^2$ and $\Omega_\varepsilon = [-\varepsilon, \varepsilon]^2 \times [-\varepsilon, \varepsilon]^2$, then

$$I_\alpha = \int_{\Omega_\varepsilon} \frac{1}{D^\alpha} + \int_{\Omega_L \setminus \Omega_\varepsilon} \frac{1}{D^\alpha} =: J_\alpha^\varepsilon + k_\varepsilon \geq J_\alpha^\varepsilon$$

with $0 < k_\varepsilon < +\infty$ since $D^\alpha$ is bounded away from $\Omega_\varepsilon$. Therefore $J_\varepsilon^\alpha \leq I_\alpha = J_\alpha^\varepsilon + k_\varepsilon$ and then $I_\alpha$ is divergent iff $J_\alpha^\varepsilon$ is divergent. Now, as before,

$$|X - Y|^2 = (x + r\sin\varphi)^2 + (y - r\sin\theta)^2 + (r(1 - \cos\theta) + r(1 - \cos\varphi))^2$$

and setting $\xi = x/r$, $\eta = y/r$, $J_\alpha^\varepsilon$ reduces to

$$J_\alpha^\varepsilon = \int\limits_{[-\varepsilon,\varepsilon]^4} \frac{r^{2-\alpha}\, \mathrm{d}\varphi\, \mathrm{d}\theta\, \mathrm{d}\xi\, \mathrm{d}\eta}{\left((\xi + \sin\varphi)^2 + (\eta - \sin\theta)^2 + ((1 - \cos\theta) + (1 - \cos\varphi))^2\right)^{\frac{\alpha}{2}}} \tag{19}$$

We study now when $J_\alpha^\varepsilon$ diverges. We have

$$\begin{aligned}(2 - \cos\theta - \cos\varphi)^2 &= 4\left(\sin^2\frac{\theta}{2} + \sin^2\frac{\varphi}{2}\right)^2 \\ &\leq 4\left(\frac{\theta^2}{4} + \frac{\varphi^2}{4}\right) \leq \theta^2 + \varphi^2\end{aligned}$$

By the change of coordinates

$$u = \xi + \sin\varphi, \quad v = \eta - \sin\theta, \quad z = \varphi, \quad t = \theta$$

with Jacobian determinant equal to 1, $J_\alpha^\varepsilon$ satisfies

$$J_\alpha^\varepsilon \geq \int \frac{r^{2-\alpha}}{(u^2 + v^2 + z^2 + t^2)^{\frac{\alpha}{2}}}\, \mathrm{d}z\, \mathrm{d}t\, \mathrm{d}u\, \mathrm{d}v$$

where the integration is carried out on the domain in which $u, v \in [-\varepsilon - \sin\varepsilon, \varepsilon + \sin\varepsilon] \supseteq [-\varepsilon, \varepsilon]$, $z, t \in [-\varepsilon, \varepsilon]$. Thus,

$$J_\alpha^\varepsilon \geq \iint\limits_{[-\varepsilon,\varepsilon]^2} \iint_{C_\varepsilon} \frac{r^{2-\alpha}}{(A^2 + z^2 + t^2)^{\frac{\alpha}{2}}}\, dz\, dt\, du\, dv \tag{20}$$

with $A^2 = u^2 + v^2$ and $C_\varepsilon = \{(z, t) : z^2 + t^2 \leq \varepsilon^2\}$. The integral on $C_\varepsilon$ is easy to compute using an expansion and yields for $\alpha \neq 2$ (the case $\alpha = 2$ was treated in

Theorem 4)

$$\frac{2\pi r^{2-\alpha}}{(2-\alpha)}A^{2-\alpha}\left(\left(1+\frac{\varepsilon^2}{A^2}\right)^{\frac{2-\alpha}{2}}-1\right)$$
$$\geq \pi r^{2-\alpha}\frac{\varepsilon^2}{A^\alpha}\left(1+o\left(\frac{\varepsilon^2}{A^\alpha}\right)\right)\geq c_\varepsilon r^{2-\alpha}\frac{\pi\varepsilon^2}{(u^2+v^2)^{\frac{\alpha}{2}}}$$

for a suitable $c_\varepsilon > 0$ and $\varepsilon$ sufficiently small. Thus,

$$J_\alpha^\varepsilon \geq c_\varepsilon \pi \varepsilon^2 r^{2-\alpha}\int_{-\varepsilon}^{\varepsilon}\int_{-\varepsilon}^{\varepsilon}\frac{1}{(u^2+v^2)^{\frac{\alpha}{2}}}\,\mathrm{d}u\,\mathrm{d}v \tag{21}$$

which is easily seen to be divergent if $\alpha - 1 \geq 1$, i.e. $\alpha \geq 2$.

To discuss convergence, we neglect the term $(2-\cos\theta-\cos\varphi)^2$ in the denominator in (19) and we have

$$J_\alpha^\varepsilon \leq \int_{[-\varepsilon,\varepsilon]^4}\frac{r^{2-\alpha}\,\mathrm{d}\varphi\,\mathrm{d}\theta\,\mathrm{d}\xi\,\mathrm{d}\eta}{\left((\xi+\sin\varphi)^2+(\eta-\sin\theta)^2\right)^{\frac{\alpha}{2}}};$$

By the same coordinate change as above using as domain a circle of radius $\sqrt{2}\varepsilon$ (i.e. larger than the square of edge $2\varepsilon$), and using polar coordinates, this turns into

$$J_\alpha^\varepsilon \leq r^{2-\alpha}\int_{[-\varepsilon,\varepsilon]^2}\iint_{C_{\sqrt{2}\varepsilon}}\frac{1}{(u^2+v^2)^{\frac{\alpha}{2}}}\,\mathrm{d}u\,\mathrm{d}v\,\mathrm{d}z\,\mathrm{d}t$$
$$\leq 8\pi\varepsilon^2 r^{2-\alpha}\int_0^{\sqrt{2}\varepsilon}\frac{1}{\sigma^{\alpha-1}}\,\mathrm{d}\sigma$$

by an analogous reasoning as above. So, $J_\alpha^\varepsilon$ converges (if there is only one point of self-contact) if $\alpha < 2$.

It remains to investigate when the integral diverges if there is a line of points of contact on bd $T_r$. Without loss of generality, we can suppose to have contact between two parallel cylinders of length $L$ along the $x$-axis. With analogous notation as above, we have $X(x_1, r\sin\theta, r(1-\cos\theta))$ and $Y(x_2, r\sin\varphi, -r(1-\cos\varphi))$ and

$$\|X-Y\|^2 = (x_1-x_2)^2 + r^2(\sin\theta-\sin\varphi)^2 + r^2(2-\cos\theta-\cos\varphi)^2.$$

Now it is no more possible to restrict to $[-\varepsilon,\varepsilon]^2$ on the $(x_1, x_2)$ coordinates, but still on the angles. Then $I_\alpha$ will diverge if

$$J_\alpha^\varepsilon = \iint_{[-L,L]^2}\iint_{[-\varepsilon,\varepsilon]^2}\frac{\mathrm{d}x_1\,\mathrm{d}x_2\,\mathrm{d}\theta\,\mathrm{d}\varphi}{[(x_1-x_2)^2+(\sin\theta-\sin\varphi)^2+(2-\cos\theta-\cos\varphi)^2]^{\alpha/2}}$$

diverges. With the same reasoning as above, it is easy to see that if $\varepsilon$ is small enough, then

$$J_\alpha^\varepsilon \geq \iint_{[-L,L]^2} \iint_{[-\varepsilon,\varepsilon]^2} \frac{C}{(B^2+\theta^2+\varphi^2)^{\alpha/2}}\,\mathrm{d}x_1\,\mathrm{d}x_2\,\mathrm{d}\theta\,\mathrm{d}\varphi$$

where $B^2 = (x_1 - x_2)^2$ and $C$ is a positive constant depending on $\varepsilon$. The right-hand side is analogous to the right-hand side of (20) and therefore, as in (21)

$$J_\alpha^\varepsilon \geq D \int_{-L}^{L}\int_{-L}^{L} \frac{1}{(x_1-x_2)^\alpha}\,\mathrm{d}x_1\,\mathrm{d}x_2$$

for a suitable positive constant $D$, including in this case also $\alpha = 2$. This is easily seen to be divergent if $\alpha \geq 1$ by switching to the coordinates $\xi = x_1 - x_2$, $\eta = x_1 + x_2$. This completes the proof. □

***Remark 8*** The above results show that if the total energy (for generic $\alpha < 3$) diverges, then this must be ascribed to the divergence of the term with the Euclidean distance if $\alpha \geq 2$ and there is at least a point of self-contact. However, in this case the divergence of the integral cannot distinguish between a single (or finite) point of contact and a line of contact. On the other side, if $1 \leq \alpha < 2$ and the integral diverges, then there must be a line of points of contact.

***Remark 9*** The result is the same as in Freedman et al. (1994) for a finite number of self-contact intersections: the admissible range for $\alpha$ is $[2, 3)$, which provides a finite energy for knots without double points and diverges in the case of loss of injectivity.

***Remark 10*** In the setting of knots, it is easy to see that in O'Hara's functional in (12) with general exponent $\alpha$, for nearby points on a circle, one is faced with the limit

$$\lim_{x\to 0} \frac{1}{2^\alpha R^\alpha \left|\sin\left(\frac{x}{2}\right)\right|^\alpha} - \frac{1}{R^\alpha x^\alpha}$$

that is finite for $\alpha \in (0, 3)$.
One could do the same on the surface of a torus with exponents $\alpha = 1, 3, 4$ (the general case is far too complicated). After long calculations that involve the expansions of incomplete and complete elliptic integrals of the first, second and third kind the limit turns out to be bounded for $\alpha = 1$ and unbounded in the other two cases, as expected.

## 8 Numerical Examples

In this Section we show the possibility of applying the functional introduced in Sect. 4 through two examples and we support with numerical results the main properties proved above. As said before, different generalizations of Möbius energy were proposed; however, they are mostly developed theoretically, while we can provide a

functional that seems easier to compute and that can be applied to a simplified model of elastic filaments.
For both the following cases, the computations were carried out with the software Wolfram Mathematica (version 13.0).

### 8.1 Modelling of a Torus with Variable Thickness

While in general this leads to elliptic integrals, to present some simple results and to have a simplified version of $d^{*2}$, we consider a planar centreline $\gamma$; by Theorem 2, we expect divergence for self-contact and interpenetration.
We then choose the centreline $\gamma$ as a circle of radius $R = 1$.
Its tubular neighbourhood $T_r$ is obviously a torus; we study the following energy functional

$$\mathcal{E}(T_r) = E(T_r) + F(T_r) = \int_0^L -\kappa r^2 \mathrm{d}s + F(T_r)$$

where $r$ can vary and the first term favours the increasing of the thickness $r$. Clearly, the minimization of this first energy term is influenced by the introduction of the functional $F(T_r)$; thus, self-contact and interpenetration of matter are avoided without restricting the space of admissible configurations.
We use the arc-length parametrization $\gamma = (\cos s, \sin s, 0), \quad s \in [0, 2\pi]$. We compute the Euclidean distance between two points $X$ and $Y$ on the surface of the torus and the minimal length along a parallel, knowing $\kappa = 1$ and $\tau = 0$.
Using the substitution $s - t = |x|$ and exploiting symmetry, we have

$$\begin{aligned}|X - Y|^2 = &-2r^2(\cos\theta\cos\varphi\cos|x| + \sin\theta\sin\varphi - 1)\\ &-2r(-\cos\theta\cos|x| - \cos\varphi\cos|x| + \cos\theta + \cos\varphi) - 2(\cos|x| - 1)\end{aligned}$$

while

$$\begin{aligned}d^{*2}(X, Y) = &\, r^2 \min(|\theta - \varphi|, ||\theta - \varphi| - 2\pi|)^2\\ &+(1 - r\cos\theta)(1 - r\cos\varphi)\min(|x|, (2\pi - |x|))^2\end{aligned}$$

The functional then reduces to

$$\begin{aligned}\mathcal{E} = &\int_0^{2\pi} -r^2 \mathrm{d}s\\ &+ 2\cdot 2\pi \int_0^{2\pi}\int_0^{2\pi}\int_0^{\pi}\left(\frac{1}{|X - Y|^2} - \frac{1}{d^{*2}(X, Y)}\right)\mathrm{d}x\,\mathrm{d}\varphi\,\mathrm{d}\theta.\end{aligned}$$

We proceed now by computing, for different values of $r$, the value of $\mathcal{E}(T_r)$, exploiting a numerical integration over $[0, 2\pi] \times [0, 2\pi] \times [0, \pi]$ for $F(T_r)$, as shown in Table 1.
In order to carry out a precise analysis for $F(T_r)$ we act with two different options in Wolfram Mathematica: the Global Adaptive Strategy (GAS) and the Local Adaptive

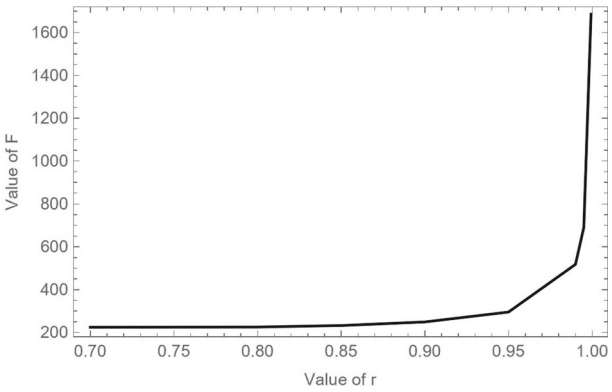


**Fig. 6** Representation of the values of $F(T_r)$ versus $r$ shown in Table 1

Strategy (LAS) with default values (we refer to Wolfram documentation for a complete description).

The application of GAS provides the estimated value and an error, so to provide a detailed analysis we apply also LAS; this method generates an error around the value 0 for $x$, then we let $x$ vary on the interval $[0 + \varepsilon, \pi - \varepsilon]$, with $\varepsilon$ varying between 0.1 and 0.0001. The result obtained with progressively increasing precision effectively tends to the one obtained with GAS.

We present now the results obtained assuming $r$ equal to different values in the interval $[0.7, 0.993]$: clearly, they do not cause interpenetration of matter or self-contact, as shown in yellow in Fig. 7. The results are reported with a precision of $10^{-2}$ for the value of the integral and $10^{-5}$ for the error of GAS.

It is easy to notice that the GAS with these values of parameters is quite precise. The behaviour of the value of $F(T_r)$ with respect to the parameter $r$ is also shown in Fig. 6 and, as one can easily see in row 6 of Table 1, it increases with $r$, i.e. it increases while we approach the value of $r$ that causes a first self-contact, that is $r = 1$. Moreover, approaching this value, the integral increases rapidly, as expected.

Setting $r = 1$, the torus presents a self-contact configuration with all the cross-sections $\mathcal{A}(s)$ meeting in the central point $(0, 0, 0)$ and the angle with the normal vector to $\gamma$ is 0, as shown in Figs. 7 and 8.

The application of LAS does not provide results because of failure in convergence after recursive bisections of the intervals over which we integrate: in particular, singularity occurs around the point $(\theta, \varphi) = (0, 0)$. Such coordinates indeed correspond to the central point of the torus, where self-contact occurs. Carrying out the computation with GAS we obtain a value of 3404.81 with an error of 438.84764. Clearly, its influence on the result cannot be ignored, but it gives anyway a hint on the behaviour of the functional, that, as expected and proven before, becomes very big.

The last case we consider is with $r = 1.1$, i.e. a configuration with interpenetration of matter as shown in Fig. 7. In this case, as before, LAS is not able to compute results on the domain $[0, \pi] \times [0, 2\pi] \times [0, \pi]$.

We then apply LAS letting $x$ vary on $[0.01, \pi - 0.01]$ and with $\theta$ and $\varphi$ in three different intervals, as shown in Table 2. For every interval, we provide a progressive

**Table 1** Results for the value of the functional for different parameters of $r$ and different methods of integration

| $r$ | 0.7 | 0.8 | 0.85 | 0.9 | 0.95 | 0.99 | 0.995 | 0.9993 |
|---|---|---|---|---|---|---|---|---|
| LAS $\varepsilon = 10^{-1}$ | 205.35 | 207.35 | 214.16 | 229.89 | 273.04 | 479.27 | 638.65 | 1550.20 |
| LAS $\varepsilon = 10^{-2}$ | 222.54 | 223.59 | 230.54 | 247.15 | 293.17 | 513.84 | 684.50 | 1661.24 |
| LAS $\varepsilon = 10^{-3}$ | 224.31 | 225.25 | 232.22 | 248.90 | 295.22 | 517.38 | 689.21 | 1673.26 |
| LAS $\varepsilon = 10^{-4}$ | 224.48 | 225.41 | 232.39 | 249.08 | 295.42 | 517.75 | 689.64 | 1682.35 |
| GAS | 224.50 | 225.44 | 232.41 | 249.11 | 295.44 | 518.17 | 690.89 | 1686.23 |
| GAS error | 0.00119 | 0.00214 | 0.00301 | 0.00523 | 0.01125 | 0.10818 | 0.05995 | 5.83014 |
| $E(T_r)$ | −3.08 | −4.02 | −4.54 | −5.09 | −5.67 | −6.16 | −6.22 | −6.27 |
| $\mathcal{E}(T_r)$ | 221.42 | 221.41 | 227.87 | 244.02 | 289.77 | 512.01 | 684.77 | 1679.96 |

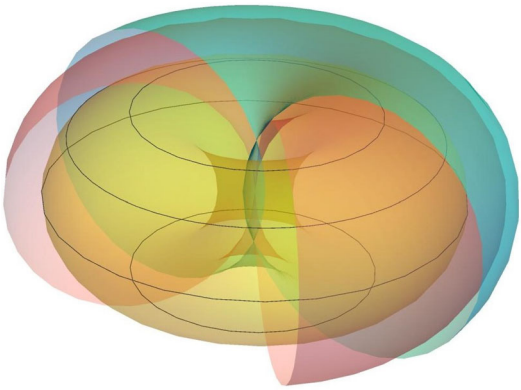

**Fig. 7** Representation of the torus with $r = 0.7, 1, 1.1$, respectively in yellow, pink for self-contact configuration and light blue for configuration with interpenetration

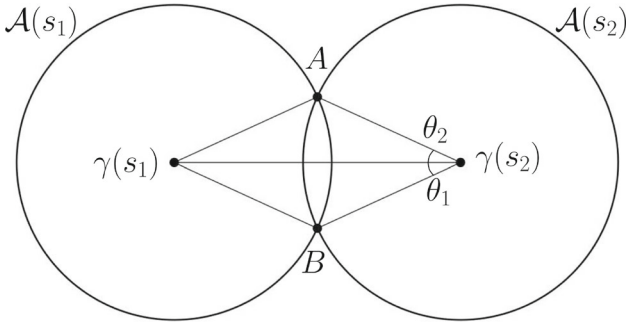


**Fig. 8** Representation of the angles for which we have divergence in the case of interpenetration

refinement in three steps enlarging its width towards two values around which the integration process diverges. This values are approximately $\theta_1 \sim 0.4297$ and $\theta_2 = -\theta_1 \sim 2\pi - 0.4297 = 5.85349$, that are exactly the two angles, as shown in Fig. 8, that determine the points $A$ and $B$ in which two generic cross-sections overlap. Thus, as expected, we obtain finite results that increase rapidly when we approach the two precise values $\theta_1$ and $\theta_2$.
Using GAS, we obtain 10943.92 with an error of 1418.77361. As before, the error affects the result, but it is however in accordance with our expectations.

On the other hand, setting $r = 0$ and integrating we obtain the value 4, as for Möbius energy on a circle. We remark that, as proven before, all the values obtained are positive. Coupling the results of $F(T_r)$ with $E(T_r)$, it is clear that the minimum of $\mathcal{E}(T_r)$ (if it exists) cannot be attained by high values of $r$, as expected. The term $F(T_r)$ acts as a physical constraint, interacting with $E(T_r)$, without the necessity of limiting the space of admissible configurations with geometric constraints, often difficult to express globally: our definition automatically detects both local or global interpenetration of matter.

**Table 2** Results for $F(T_r)$ with $r = 1.1$ and different intervals for $\theta$ and $\varphi$

| Interval for $\theta$ | $F(T_r)$ |
|---|---|
| [0, 0.428] | 2438.32 |
| [0, 0.429] | 2799.83 |
| [0, 0.4296] | 3590.72 |
| [0.431, 5.852] | 260.294 |
| [0.430, 5.853] | 280.574 |
| [0.4298, 5.8534] | 365.974 |
| [5.855, $2\pi$] | 2485.18 |
| [5.854, $2\pi$] | 2924.39 |
| [5.8535, $2\pi$] | 4342.54 |

The value of $F[T_r]$ can be obtained summing the result on the three intervals. In every triple, the first row is the less refined interval, while the last is the most refined

### 8.2 Modelling an Arc of Helix with Variable Thickness

In order to show an example with a non-simplified $d^{*2}$, we compute the values of $F(T_r)$ with $T_r$ a tube, where a part of it is made up of the tubular neighbourhood of an helix, which we take for simplicity with open ends. The helix is parametrized by the arclength, so

$$\gamma = \left( R\cos\left(\frac{s}{\sqrt{a^2+R^2}}\right), R\sin\left(\frac{s}{\sqrt{a^2+R^2}}\right), \frac{as}{\sqrt{a^2+R^2}}\right)$$

where $s \in [0, 7\pi]$, with $7\pi < L/2$, with $L$ the length of the centreline of $T_r$.
The curvature and torsion are

$$\kappa = \frac{R}{a^2+R^2} \qquad \tau = \frac{a}{a^2+R^2}.$$

Given two points $X$ and $Y$ on the surface of the torus, using the substitution $s - t = |x|$ and proceeding by symmetry, we easily compute $|X - Y|^2$ (that we omit here for the sake of brevity), while

$$d^{*2}(X,Y) = \left( r\min(|\theta-\varphi|, ||\theta-\varphi| - 2\pi|) + r\left|\frac{ax}{a^2+R^2}\right|\right)^2 + \frac{|x|^2\left(a^2 - rR\cos(\theta)+R^2\right)\left(a^2 - rR\cos(\varphi)+R^2\right)}{\left(a^2+R^2\right)^2}$$

where we do not consider the shortest length of the parallel because of the hypothesis that we are considering less than a half of the curve $\gamma$.

**Table 3** Results for the value of the functional for different parameters of $r$ and different methods of integration

| $r$ | 2 | 2.5 | 2.9 | 3 | 3.3 |
|---|---|---|---|---|---|
| LAS $\varepsilon = 10^{-2}$ | 4153.43 | 4261.318 | 5109.59 | 5678.2 | 13350.82 |
| LAS $\varepsilon = 10^{-3}$ | 5379.22 | 5449.58 | 6491.96 | 7192.35 | 17543.04 |
| LAS $\varepsilon = 10^{-4}$ | 6598.7 | 6632.09 | 7867.23 | 8689 | 21311.3 |
| LAS $\varepsilon = 10^{-5}$ | 7798.16 | 7806.11 | 9239.57 | 10618.8 | 24419.64 |

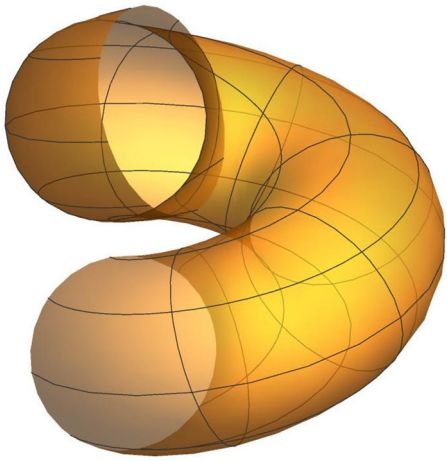

**Fig. 9** Representation of the arc of helix with $r = 2.5$

The functional then becomes

$$\mathcal{E} = 2 \cdot (7\pi) \int_0^{2\pi} \int_0^{2\pi} \int_0^{7\pi} \left( \frac{1}{|X - Y|^2} - \frac{1}{d^{*2}(X, Y)} \right) \mathrm{d}x \, \mathrm{d}\varphi \, \mathrm{d}\theta$$

We proceed as before by integrating numerically on $x, \theta, \varphi$, letting $r$ vary in $[2, 3.3]$. We choose $R = 3, a = 1$, while the interval of $s$ is chosen to have at least a complete turn around the $z$-axis.

The Global Adaptive Strategy is strongly affected by errors; thus, we apply the LAS with different progressive types of precision on the interval $[\varepsilon, 7\pi - \varepsilon]$. The results are reported in Table 3. As one can see in Fig. 11, we plot the behaviours of the results, for different approximations of $F(T_r)$, depending on the value of $\varepsilon$, with a progression towards the top from less to most accurate. The graphs show high accordance, thus we believe that we can generalize this study to the case with $\varepsilon = 0$, i.e. the precise functional $F(T_r)$.

The results are computed without errors and behave as expected, with divergence in values of $r$ greater than 3, around which, as one can see from Figs. 9, 10, the helix starts presenting self-contact or interpenetration.

A precise analysis of possible self-contact points is on the other hand much more complicate: to find the radius $r$ for which a self-contact occurs after a first turn between

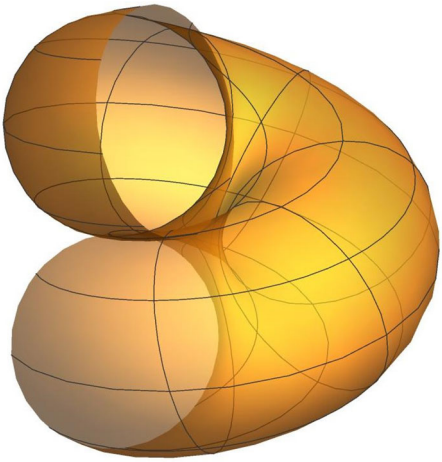

**Fig. 10** Representation of the arc of helix with $r = 3$

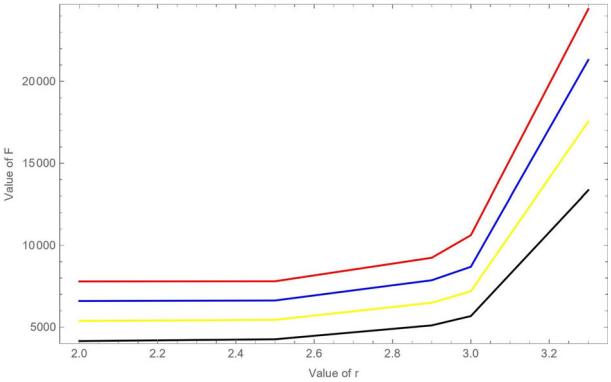


**Fig. 11** Representation of the values of $F(T_r)$ versus $r$ shown in Table 3. In black, $\varepsilon = 10^{-2}$; in yellow, $\varepsilon = 10^{-3}$, in blue, $\varepsilon = 10^{-4}$, in red, $\varepsilon = 10^{-5}$

an unknown section at abscissa $s$ and the cross-section with $s = 0$ between the upper and lower part of the helix, one must write the generic vector $\gamma(s) - \gamma(0)$, that turns out to be

$$\left(R\cos\left(\frac{s}{\sqrt{a^2+R^2}}\right) - R,\, R\sin\left(\frac{s}{\sqrt{a^2+R^2}}\right),\, \frac{as}{\sqrt{a^2+R^2}}\right)$$

and study for which $s$ this is orthogonal to $\boldsymbol{t}(0) = \left(0, \frac{R}{\sqrt{a^2+R^2}}, \frac{a}{\sqrt{a^2+R^2}}\right)$. Indeed, as explained in Lonati and Marzocchi (2024), an orthogonality condition holds between the vector that joins two central points of the cross-sections that overlap, i.e. $\gamma(0)$ and $\gamma(s)$, and the tangent vectors $\boldsymbol{t}(0)$ and $\boldsymbol{t}(s)$. Knowing $R = 3$ and $a = 1$, we obtain $s = 5.65\pi$; in addition, we know that the distance between the two centres must be equal to $2r$, so,

$$\left(R\cos\left(\frac{s}{\sqrt{a^2+R^2}}\right)-R\right)^2+\left(R\sin\left(\frac{s}{\sqrt{a^2+R^2}}\right)\right)^2+\left(\frac{as}{\sqrt{a^2+R^2}}\right)^2=4r^2$$

and from this equality we numerically obtain $r = 2.975$ as critical thickness, that supports our results. We remark that with these parameters of $R$ and $a$, a first contact in the inner part of the helix (on $z$-axis) corresponds to $r = 3.43$, so it is not detected because this inner contact happens after the other contact due to a complete turn of the helix. We underline that the study of the functional here provides much faster results and simpler computations, instead of the procedure required to find the precise value of $r$ just for the contact with the section $\mathcal{A}(0)$.

## Appendix A Computations for the Proof of Theorem 3

$$\begin{aligned}
A_3 &= \eta_1^2(\eta_2 r^2\tau'(s)\cos^2\theta+\eta_2\kappa(s)r\sin\theta-\eta_2\kappa(s)^2r^2\cos\theta\sin\theta+\eta_2 r^2\tau'(s)\sin^2\theta)\\
&\quad+\eta_1^3(-\kappa'(s)r\cos\theta+\kappa(s)\kappa'(s)r^2\cos^2\theta+r^2\tau'(s)\tau(s)\cos^2\theta+r^2\tau'(s)\tau(s)\sin^2\theta);\\
A_4 &= \eta_1^4\left(\frac{1}{3}\kappa''(s)\kappa(s)r^2\cos^2\theta-\frac{1}{3}\kappa''(s)r\cos\theta-\frac{1}{12}\kappa(s)^4r^2\cos^2\theta+\frac{1}{6}\kappa(s)^3r\cos\theta\right.\\
&\quad-\frac{1}{12}\kappa(s)^2r^2\tau(s)^2\sin^2\theta-\frac{1}{6}\kappa(s)^2r^2\tau(s)^2\cos^2\theta-\frac{1}{6}\kappa(s)^2r^2\tau'(s)\sin\theta\cos\theta-\frac{\kappa(s)^2}{12}\\
&\quad+\frac{1}{6}\kappa(s)\kappa'(s)r^2\tau(s)\sin\theta\cos\theta+\frac{1}{6}\kappa(s)r\tau'(s)\sin\theta+\frac{1}{6}\kappa(s)r\tau(s)^2\cos\theta\\
&\quad\left.+\frac{1}{4}\kappa'(s)^2r^2\cos^2\theta+\frac{1}{3}r^2\tau''(s)\tau(s)\sin^2\theta-\frac{r^2\tau(s)^4}{12}+\frac{r^2\tau'(s)^2}{4}\right)\\
&\quad+\eta_1^3\left(-\frac{1}{3}\eta_2\kappa(s)^2r^2\tau(s)-\eta_2\kappa(s)\kappa'(s)r^2\sin\theta\cos\theta+\frac{1}{3}\eta_2\kappa(s)r\tau(s)\cos\theta\right.\\
&\quad\left.+\frac{2}{3}\eta_2\kappa'(s)r\sin\theta-\frac{1}{3}\eta_2r^2\tau(s)^3+\frac{1}{3}\eta_2r^2\tau''(s)\sin^2\theta\right)\\
&\quad+\eta_1^2\left(-\frac{1}{2}\eta_2^2\kappa(s)^2r^2\cos^2\theta+\frac{1}{2}\eta_2^2\kappa(s)r\cos\theta-\frac{1}{2}\eta_2^2r^2\tau(s)^2\right)-\frac{1}{3}\eta_1\eta_2^3r^2\tau(s)-\frac{\eta_2^4r^2}{12};\\
B_4 &= \eta_1^4\left(\frac{1}{3}\kappa''(s)\kappa(s)r^2\cos^2\theta-\frac{1}{3}\kappa''(s)r\cos\theta+\frac{1}{4}\kappa'(s)^2r^2\cos^2\theta+\frac{1}{3}r^2\tau''(s)\tau(s)\right.\\
&\quad\left.+\frac{r^2\tau'(s)^2}{4}\right)+\eta_1^3\left(-\eta_2\kappa(s)\kappa'(s)r^2\sin\theta\cos\theta+\frac{1}{2}\eta_2\kappa'(s)r\sin\theta+\frac{1}{3}\eta_2r^2\tau''(s)\right)\\
&\quad+\eta_1^2\left(\frac{1}{2}\eta_2^2\kappa(s)r\cos\theta-\frac{1}{2}\eta_2^2\kappa(s)^2r^2\cos^2\theta\right).
\end{aligned}$$

**Acknowledgements** The authors thank Francesco Ballarin for his helpful suggestions for the computations of Sect. 8. CL and AM are supported by Gruppo Nazionale per la Fisica Matematica (GNFM) of Istituto Nazionale per l'Alta Matematica (INdAM).

**Funding** Open access funding provided by Università Cattolica del Sacro Cuore within the CRUI-CARE Agreement.

**Data Availability** The manuscript has no associated data.

## Declarations

**Conflict of interest** On behalf of all authors, the corresponding author states that there is no conflict of interest.



## References

Adams, C.C.: The Knot Book: An Elementary Introduction to the Mathematical Theory of Knots. W. H. Freeman & Company, New York (1994)

Antman, S.: Nonlinear Problems of Elasticity, vol. 107. Applied Mathematical Sciences, 2nd edn. Springer, New York (2005)

Ballarin, F., Bevilacqua, G., Lussardi, L., Marzocchi, A.: Elastic membranes spanning deformable boundaries. ZAMM (2024). https://doi.org/10.1002/zamm.202300890

Bevilacqua, G., Lonati, C.: Effects of surface tension and elasticity on critical points of the Kirchhoff–Plateau problem. Bollettino dell'Unione Matematica Italiana **17**, 221–240 (2023). https://doi.org/10.1007/s40574-023-00392-6

Bevilacqua, G., Lussardi, L., Marzocchi, A.: Soap film spanning electrically repulsive elastic protein links. Atti della Accademia Peloritana dei Pericolanti-Classe di Scienze Fisiche, Matematiche e Naturali (2018). https://doi.org/10.1478/AAPP.96S3A

Bevilacqua, G., Lussardi, L., Marzocchi, A.: Soap film spanning an elastic link. Q. Appl. Math. **77**(3), 507–523 (2019). https://doi.org/10.1090/qam/1510

Bevilacqua, G., Lussardi, L., Marzocchi, A.: Dimensional reduction of the Kirchhoff–Plateau problem. J. Elast. **140**, 135–148 (2020). https://doi.org/10.1007/s10659-020-09763-y

Bevilacqua, G., Lussardi, L., Marzocchi, A.: Variational analysis of inextensible elastic curves. Proc. R. Soc. A **478**(2260), 20210741 (2022). https://doi.org/10.1098/rspa.2021.0741

Bishop, R.L.: There is more than one way to frame a curve. Am. Math. Mon. **82**(3), 246–251 (1975). https://doi.org/10.2307/2319846

Buck, G., Orloff, J.: A simple energy function for knots. Topol. Appl. **61**(3), 205–214 (1995). https://doi.org/10.1016/0166-8641(94)00024-W

Burde, G., Zieschang, H.: Knots. de Gruyter Studies in Mathematics, Berlin (2003)

Chamekh, M., Mani-Aouadi, S., Moakher, M.: Modeling and numerical treatment of elastic rods with frictionless self-contact. Comput. Methods Appl. Mech. Eng. **198**(47–48), 3751–3764 (2009). https://doi.org/10.1016/j.cma.2009.08.005

Chamekh, M., Latrach, M.A., Renard, Y.: Frictional self-contact problem of elastic rods. J. King Saud Univ. Sci. **32**(1), 828–835 (2020). https://doi.org/10.1016/j.jksus.2019.02.017

Ciarlet, P.G., Nečas, J.: Injectivity and self-contact in nonlinear elasticity. Arch. Ration. Mech. Anal. **97**(3), 171–188 (1987). https://doi.org/10.1007/BF00250807

Crowell, R.H., Fox, R.H.: Introduction to Knot Theory, vol. 57. Springer, New York (2012)

De Rosa, A., Lussardi, L.: On the anisotropic Kirchhoff–Plateau problem. Math. Eng. **4**(2), 1–13 (2022). https://doi.org/10.3934/mine.2022011

Freedman, M.H., He, Z.-X., Wang, Z.: Möbius energy of knots and unknots. Ann. Math. **139**(1), 1–50 (1994). https://doi.org/10.2307/2946626

Giusteri, G.G., Franceschini, P., Fried, E.: Instability paths in the Kirchhoff–Plateau problem. J. Nonlinear Sci. **26**, 1097–1132 (2016). https://doi.org/10.1007/s00332-016-9299-4

Giusteri, G.G., Lussardi, L., Fried, E.: Solution of the Kirchhoff–Plateau problem. J. Nonlinear Sci. **27**, 1043–1063 (2017). https://doi.org/10.1007/s00332-017-9359-4

Gonzalez, O., Maddocks, J.H.: Global curvature, thickness, and the ideal shapes of knots. Proc. Natl. Acad. Sci. **96**(9), 4769–4773 (1999). https://doi.org/10.1073/pnas.96.9.4769
Gonzalez, O., Maddocks, J.H., Schuricht, F., Mosel, H.V.D.: Global curvature and self-contact of nonlinearly elastic curves and rods. Calc. Var. Partial Differ. Equ. **14**, 29–68 (2002). https://doi.org/10.1007/s005260100089
Käfer, B., Mosel, H.: Möbius-invariant self-avoidance energies for non-smooth sets of arbitrary dimension and co-dimension. Adv. Math. **426**, 109108 (2023)
Kim, D., Kusner, R.: Torus knots extremizing the möbius energy. Exp. Math. **2**(1), 1–9 (1993)
Kusner, R., Sullivan, J.: Möbius energies for knots and links, surfaces and submanifolds. Ann. Math. (2) **139**(1), 1–50 (1994)
Kusner, R., Sullivan, J.: On distortion and thickness of knots. In: Topology and Geometry in Polymer Science, pp. 67–76. Springer, New York (1998). https://doi.org/10.1007/978-1-4612-1712-1_7
Litherland, R.A., Simon, J., Durumeric, O., Rawdon, E.: Thickness of knots. Topol. Appl. **91**(3), 233–244 (1999). https://doi.org/10.1016/S0166-8641(97)00210-1
Lonati, C., Marzocchi, A.: On self-contact and non-interpenetration of elastic rods. Math. Mech. Solids (2024). https://doi.org/10.1177/10812865231226311
Mlika, R.: Nitsche method for frictional contact and self-contact: mathematical and numerical study (2018)
Mosel, H.: Elastic knots in euclidean 3-space. In: Annales de l'Institut Henri Poincaré C, Analyse Non Linéaire, vol. 16, pp. 137–166. Elsevier (1999). https://doi.org/10.1016/S0294-1449(99)80010-9
Mosel, H.: Minimizing the elastic energy of knots. Asymptot. Anal. **18**(1–2), 49–65 (1998)
O'Hara, J.: Energy of a knot. Topology **30**(2), 241–247 (1991). https://doi.org/10.1016/0040-9383(91)90010-2
O'Hara, J.: Family of energy functionals of knots. Topol. Appl. **48**(2), 147–161 (1992). https://doi.org/10.1016/0166-8641(92)90023-S
O'Hara, J.: Energy functionals of knots: second part. Topol. Appl. **56**(1), 45–61 (1994). https://doi.org/10.1016/0166-8641(94)90108-2
O'Hara, J.: Energy of knots and the infinitesimal cross ratio. Geom. Topol. Monogr. **13**, 421–445 (2008). https://doi.org/10.2140/gtm.2008.13.421
O'Hara, J.: Self-repulsiveness of energies for closed submanifolds. Math. Nachr. **296**(2), 797–810 (2023). https://doi.org/10.1002/mana.202000158
Rawdon, E.J., Simon, J.: Möbius energy of thick knots. Topol. Appl. **125**(1), 97–109 (2002). https://doi.org/10.1016/S0166-8641(01)00263-2
Schuricht, F.: Global injectivity and topological constraints for spatial nonlinearly elastic rods. J. Nonlinear Sci. **12**(5), 423–444 (2002). https://doi.org/10.1007/s00332-002-0462-8
Schuricht, F., Mosel, H.V.D.: Euler–Lagrange equations for nonlinearly elastic rods with self-contact. Arch. Ration. Mech. Anal. **168**, 35–82 (2003). https://doi.org/10.1007/s00205-003-0253-x
Schuricht, F., Mosel, H.: Characterization of ideal knots. Calc. Var. Partial. Differ. Equ. **19**(3), 281–305 (2004). https://doi.org/10.1007/s00526-003-0216-y
Simon, J.: Energy functions for knots: beginning to predict physical behavior. In: Mathematical Approaches to Biomolecular Structure and Dynamics, pp. 39–58. Springer, New York (1996). https://doi.org/10.1007/978-1-4612-4066-2_4
Strzelecki, P., Von Der Mosel, H.: Integral menger curvature for surfaces. Adv. Math. **226**(3), 2233–2304 (2011). https://doi.org/10.1016/j.aim.2010.09.016